

## Common Variants Within Oxidative Phosphorylation Genes Influence Risk of Ischemic Stroke and Intracerebral Hemorrhage

Christopher D. Anderson, Alessandro Biffi, Michael A. Nalls, William J. Devan, Kristin Schwab, Alison M. Ayres, Valerie Valant, Owen A. Ross, Natalia S. Rost, Richa Saxena, Anand Viswanathan, Bradford B. Worrall, Thomas G. Brott, Joshua N. Goldstein, Devin Brown, Joseph P. Broderick, Bo Norrving, Steven M. Greenberg, Scott L. Silliman, Björn M. Hansen, David L. Tirschwell, Arne Lindgren, Agnieszka Slowik, Reinhold Schmidt, Magdy Selim, Jaume Roquer, Joan Montaner, Andrew B. Singleton, Chelsea S. Kidwell, Daniel Woo, Karen L. Furie, James F. Meschia and Jonathan Rosand  
on behalf of the International Stroke Genetics Consortium

*Stroke*. 2013;44:612-619; originally published online January 29, 2013;  
doi: 10.1161/STROKEAHA.112.672089

*Stroke* is published by the American Heart Association, 7272 Greenville Avenue, Dallas, TX 75231  
Copyright © 2013 American Heart Association, Inc. All rights reserved.  
Print ISSN: 0039-2499. Online ISSN: 1524-4628

The online version of this article, along with updated information and services, is located on the World Wide Web at:

<http://stroke.ahajournals.org/content/44/3/612>

Data Supplement (unedited) at:

<http://stroke.ahajournals.org/content/suppl/2013/01/29/STROKEAHA.112.672089.DC1.html>

**Permissions:** Requests for permissions to reproduce figures, tables, or portions of articles originally published in *Stroke* can be obtained via RightsLink, a service of the Copyright Clearance Center, not the Editorial Office. Once the online version of the published article for which permission is being requested is located, click Request Permissions in the middle column of the Web page under Services. Further information about this process is available in the [Permissions and Rights Question and Answer](#) document.

**Reprints:** Information about reprints can be found online at:  
<http://www.lww.com/reprints>

**Subscriptions:** Information about subscribing to *Stroke* is online at:  
<http://stroke.ahajournals.org/subscriptions/>

# Common Variants Within Oxidative Phosphorylation Genes Influence Risk of Ischemic Stroke and Intracerebral Hemorrhage

Christopher D. Anderson, MD\*; Alessandro Biffi, MD\*; Michael A. Nalls, PhD; William J. Devan, BS; Kristin Schwab, BA; Alison M. Ayres, BA; Valerie Valant, BA; Owen A. Ross, PhD; Natalia S. Rost, MD; Richa Saxena, PhD; Anand Viswanathan, MD; Bradford B. Worrall, MD, MSc; Thomas G. Brott, MD; Joshua N. Goldstein, MD; Devin Brown, MD; Joseph P. Broderick, MD; Bo Norrving, MD; Steven M. Greenberg, MD, PhD; Scott L. Silliman, MD; Björn M. Hansen, BS; David L. Tirschwell, MD; Arne Lindgren, MD; Agnieszka Slowik, MD; Reinhold Schmidt, MD; Magdy Selim, MD; Jaume Roquer, MD, PhD; Joan Montaner, MD, PhD; Andrew B. Singleton, PhD; Chelsea S. Kidwell, MD; Daniel Woo, MD; Karen L. Furie, MD; James F. Meschia, MD; Jonathan Rosand, MD, MSc; on behalf of the International Stroke Genetics Consortium

**Background and Purpose**—Previous studies demonstrated association between mitochondrial DNA variants and ischemic stroke (IS). We investigated whether variants within a larger set of oxidative phosphorylation (OXPHOS) genes encoded by both autosomal and mitochondrial DNA were associated with risk of IS and, based on our results, extended our investigation to intracerebral hemorrhage (ICH).

**Methods**—This association study used a discovery cohort of 1643 individuals, a validation cohort of 2432 individuals for IS, and an extension cohort of 1476 individuals for ICH. Gene-set enrichment analysis was performed on all structural OXPHOS genes, as well as genes contributing to individual respiratory complexes. Gene-sets passing gene-set enrichment analysis were tested by constructing genetic scores using common variants residing within each gene. Associations between each variant and IS that emerged in the discovery cohort were examined in validation and extension cohorts.

**Results**—IS was associated with genetic risk scores in OXPHOS as a whole (odds ratio [OR], 1.17;  $P=0.008$ ) and complex I (OR, 1.06;  $P=0.050$ ). Among IS subtypes, small vessel stroke showed association with OXPHOS (OR, 1.16;  $P=0.007$ ), complex I (OR, 1.13;  $P=0.027$ ), and complex IV (OR, 1.14;  $P=0.018$ ). To further explore this small vessel association, we extended our analysis to ICH, revealing association between deep hemispheric ICH and complex IV (OR, 1.08;  $P=0.008$ ).

**Conclusions**—This pathway analysis demonstrates association between common genetic variants within OXPHOS genes and stroke. The associations for small vessel stroke and deep ICH suggest that genetic variation in OXPHOS influences small vessel pathobiology. Further studies are needed to identify culprit genetic variants and assess their functional consequences. (*Stroke*. 2013;44:612-619.)

**Key Words:** genes ■ mitochondria ■ OXPHOS ■ stroke

Received July 30, 2012; final revision received November 9, 2012; accepted December 19, 2012.

From the Center for Human Genetic Research, Massachusetts General Hospital, Boston, MA (C.D.A., A.B., W.J.D., V.V., N.S.R., R.S., K.L.F., J.R.); Department of Neurology, Massachusetts General Hospital, Boston, MA (C.D.A., A.B., W.J.D., V.V., N.S.R., A.V., S.M.G., K.L.F., J.R.); Hemorrhagic Stroke Research Group, Massachusetts General Hospital, Boston, MA (C.D.A., A.B., W.J.D., K.S., A.M.A., V.V., N.S.R., A.V., J.N.G., S.M.G., J.R.); Program in Medical and Population Genetics, Broad Institute, Cambridge, MA (C.D.A., A.B., W.J.D., V.V., N.S.R., R.S., J.R.); Department of Neurogenetics, Intramural Research Program, National Institute on Aging, Bethesda, MD (M.A.N., A.B.S.); Department of Neuroscience, Mayo Clinic, Jacksonville, FL (O.A.R.); Department of Neurology and Public Health Sciences, University of Virginia Health System, Charlottesville, VA (B.B.W.); Department of Neurology, Mayo Clinic, Jacksonville, FL (T.G.B., J.F.M.); Department of Emergency Medicine, Massachusetts General Hospital, Boston, MA (J.N.G.); Stroke Program, Department of Neurology, University of Michigan Health System, Ann Arbor, MI (D.B.); Department of Neurology, University of Cincinnati College of Medicine, Cincinnati, OH (J.P.B., D.W.); Department of Clinical Sciences Lund, Neurology, Lund University, Lund, Sweden (B.N., B.M.H., A.L.); Department of Neurology, Skåne University Hospital, Lund, Sweden (B.N., B.M.H., A.L.); Department of Neurology, University of Florida College of Medicine, Jacksonville, FL (S.L.S.); Stroke Center, Harborview Medical Center, University of Washington, Seattle, WA (D.L.T.); Department of Neurology, Jagiellonian University Medical College, Krakow, Poland (A.S.); Department of Neurology, Medical University Graz, Graz, Austria (R.S.); Department of Neurology, Beth Israel Deaconess Medical Center, Boston, MA (M.S.); Neurovascular Research Unit, Department of Neurology and Program in Inflammation and Cardiovascular Disorders, Institut Municipal d'Investigació Mèdica—Hospital del Mar, Universitat Autònoma de Barcelona, Barcelona, Spain (J.R.); Neurovascular Research Laboratory and Neurovascular Unit, Institut de Recerca, Hospital Vall d'Hebron, Universitat Autònoma de Barcelona, Barcelona, Spain (J.M.); and Department of Neurology, Georgetown University Medical Center, Washington, DC (C.S.K.).

Hugh S. Markus, DM, was guest editor for this article.

\*Drs Anderson and Biffi contributed equally to this work.

**The online-only Data Supplement is available with this article at <http://stroke.ahajournals.org/lookup/suppl/doi:10.1161/STROKEAHA.112.672089/-/DC1>.**

Correspondence to Christopher D. Anderson, MD, Center for Human Genetic Research, Massachusetts General Hospital, 185 Cambridge St, CZPN 5820, Boston, MA 02114. E-mail [cdanderson@partners.org](mailto:cdanderson@partners.org)

© 2013 American Heart Association, Inc.

*Stroke* is available at <http://stroke.ahajournals.org>

DOI: 10.1161/STROKEAHA.112.672089

Despite remarkable advances in prevention, diagnosis, and treatment, stroke remains the second leading cause of death in the world, and a leading cause of disability. Although many modifiable environmental factors contribute to stroke risk, there are ample data demonstrating a genetic risk component as well.<sup>1</sup> Recent genome-wide association studies (GWAS) have demonstrated that common DNA variants influence risk of ischemic stroke (IS).<sup>2-4</sup>

A previous study demonstrated that common mitochondrial variants influence risk of IS.<sup>4</sup> The mitochondrial genome is vital to the assembly of the oxidative phosphorylation (OXPHOS) apparatus, but the majority of OXPPOS structural proteins are encoded within the autosomal genome.<sup>5</sup> The OXPPOS apparatus consists of 5 complexes that are necessary to maintain aerobic homeostasis and preserve reduction/oxidation (redox) balance in the cellular environment. Multiple rare disorders are caused by mutations of OXPPOS genes, many of which result in neurodegenerative or stroke-like phenotypes, including seizures, metabolic infarcts, and encephalomyopathies.<sup>6</sup> Additionally, OXPPOS fitness plays a role in the neuronal response to and recovery after oxidative stress.<sup>7</sup>

We hypothesized that common genetic variants in OXPPOS genes, both within the autosomal and mitochondrial genome, influence the risk of stroke. To test this hypothesis, we performed a pathway-based genetic association analysis interrogating genetic variants within OXPPOS genes. We initially performed a cumulative test of all common genetic variation within OXPPOS loci by using a gene-set enrichment analysis (GSEA) technique. This allowed us to investigate whether the OXPPOS pathway was enriched for association with stroke risk. On the basis of this analysis, we sought to ascertain and quantify the role of these variants by calculating a genetic risk score from OXPPOS genes in the Massachusetts General Hospital (MGH) IS GWAS. We then replicated this risk score association in a separate data set comprising individuals from the Ischemic Stroke Genetics Study (ISGS) and Siblings with Ischemic Stroke Study (SWISS). We then tested the same risk score in intracerebral hemorrhage (ICH) using individuals from the International Stroke Genetics Consortium ICH GWAS (ISGC ICH).

## Methods

### Subjects

Genetic data and phenotypic information were contributed by the MGH IS GWAS,<sup>8</sup> ISGS,<sup>9</sup> SWISS,<sup>10</sup> and the ISGC ICH GWAS<sup>11</sup> (Table 1). Additional control individuals for the MGH data set were contributed by the MIGen Consortium, a case-control study of genetic risk for myocardial infarction.<sup>12</sup> Hospital-based IS case and control recruitment and phenotype ascertainment were performed according to protocols described previously, and stroke subtypes were assigned by Trial of ORG 10172 in Acute Stroke Treatment (TOAST) criteria.<sup>8-10</sup> In cases in which IS subtype data were unavailable, individuals were dropped from subtype analyses but were allowed to remain in all-cause IS analyses (n=124 in MGH; n=387 in ISGS/SWISS). Multicenter hospital-based ICH case and control recruitment and phenotype ascertainment were performed according to protocols described previously.<sup>11</sup> Location of ICH was assigned by stroke neurologists based on standard criteria with central adjudication.<sup>11,13</sup> Institutional review boards from all participating centers approved the study, and all participants gave informed consent for data collection, genotyping, and analysis of genetic data.

### Genotyping and Imputation

Blood samples from MGH/MIGen were processed and genotyped using the Affymetrix 6.0 platform, whereas ISGS and SWISS were assayed with the Illumina 660 W and 1M platforms according to previously published protocols.<sup>8-10</sup> Blood samples for the ISGC ICH cases and controls were genotyped on Illumina 660 W.<sup>11</sup> For harmonization across platforms, all data sets had additional genotypes imputed using PLINK v1.07 (<http://pngu.mgh.harvard.edu/~purcell/plink>) and the International HapMap Project phase 3 reference data set (<http://www.hapmap.org>). Captured mitochondrial variants from the genotyping arrays were extracted,<sup>14</sup> and raw intensity files were inspected visually by C.D.A. and A.B. to confirm accuracy of genotype calls.

### Genomic Quality Control

For all analyzed cohorts, quality control of genotyped individuals included gender-sex discordance, filtering for missingness by individual >0.1, missingness by single nucleotide polymorphism (SNP) >0.05, and minor allele frequency (MAF) <0.01. Individuals displaying cryptic relatedness ( $\hat{p} \geq 0.125$ ) and genotypes with significant departure from Hardy-Weinberg equilibrium ( $P < 10E-5$ ) were excluded from analysis.<sup>15</sup> Autosomal imputation was performed using PLINK v1.07 after quality control filtering. Mitochondrial imputation was performed using a haplotype-based approach with reference data sets from GenBank and Mitokor after additional mtDNA-specific quality control measures (Appendix I in the online-only Data Supplement).<sup>16</sup> After imputation, SNPs were excluded with MAF <0.01 or RSQR quality index <0.3.

### OXPHOS SNP Selection

Genes encoding proteins directly involved in the OXPPOS respiratory chain were selected based on published criteria from a chemical dissection of mitochondrial function, yielding a total of 95 genes in the autosomal genome and 13 genes in the mitochondrial genome.<sup>5</sup> SNPs falling within these genes  $\pm 100$  kilobases and passing quality control filtering were extracted from the MGH and ISGS/SWISS data sets after imputation and included in the final analysis. Subanalyses were performed for genes grouped according to each OXPPOS respiratory complex, classified according to annotation in the Ensembl Genome Browser (<http://www.ensembl.org>; Tables I and II in the online-only Data Supplement).

### Population Structure and Control

Only individuals of European ancestry were analyzed in the present study. Population structures for autosomal and mitochondrial variants were assessed independently because of their significantly different inheritance patterns, using principal component (PC) analysis.<sup>16</sup> Autosomal PCs 1 through 5 were extracted for each individual and were added in association testing of autosomal SNPs until no additional reduction in genomic inflation factor could be achieved (PC1-2 in all analyses). Mitochondrial PCs 1 to 10 were extracted for each individual and were similarly added in association testing of mitochondrial SNPs until mitochondrial genomic inflation factor was minimized (PC1-5 in all analyses).

### Gene-Set Enrichment Analysis

Testing for cumulative OXPPOS pathway associations with IS risk was performed using the GSEA method,<sup>17</sup> as implemented in the GenGen v.2010Apr29 software package.<sup>18</sup> GSEA was implemented in this study as a preliminary screen of the OXPPOS pathway before generation of genetic scores and as a means to minimize the possibility of any false-positive associations. The GSEA method determines whether variants within a predefined biological pathway contain more associations with the chosen phenotype than would be expected by chance alone. For IS, GSEA testing was performed in the ISGS/SWISS cohort as a preliminary analysis before genetic score generation. GSEA was performed in the ISGS/SWISS replication

**Table 1. Study Populations**

	MGH/MIGen Cases	MGH/MIGen Controls	ISGS/SWISS Cases	ISGS/SWISS Controls	ISGC ICH Cases	ISGC ICH Controls
n	484	1159	1048	1384	928	909
Small vessel	55	...	197	...	...	...
Large artery	114	...	223	...	...	...
Cardioembolic	191	...	241	...	...	...
Deep ICH	...	...	...	...	430	...
Lobar ICH	...	...	...	...	409	...
Sex (% female)	0.39	0.41	0.43	0.52	0.52	0.51
Age at enrollment, (mean, SD)	66.5 (14.6)	47.5 (8.5)	64.8 (13.6)	66.5 (12.6)	72.4 (11.5)	73.0 (8.4)
Hypertension, %	0.62	0.55	0.64	0.34	0.71	0.55
DM 2, %	0.21	0.18	0.19	0.11	0.20	0.09
Atrial fibrillation, %	0.12	0.12	0.08	0.04	0.22	0.20
Current smoker, %	0.20	0.18	0.16	0.06	0.17	0.20
Warfarin use, %	...	...	...	...	0.08	0.03

DM 2 indicates type 2 diabetes mellitus; ICH, intracerebral hemorrhage; ISGC, International Stroke Genetics Consortium; ISGS, Ischemic Stroke Genetics Study; MGH, Massachusetts General Hospital; n, number of cases/controls; SWISS, Siblings with Ischemic Stroke Study; and ..., not applicable.

cohort rather than the MGH/MIGen discovery cohort to prevent any chance enrichment of OXPPOS association in the MGH/MIGen cohort from influencing gene-sets chosen for genetic score testing. A

separate GSEA was performed in the ISGC ICH cohort. Results are reported as a permutation-derived empirical *P* value (100 000 gene-set permutations) for gene-set association with the IS or ICH risk,

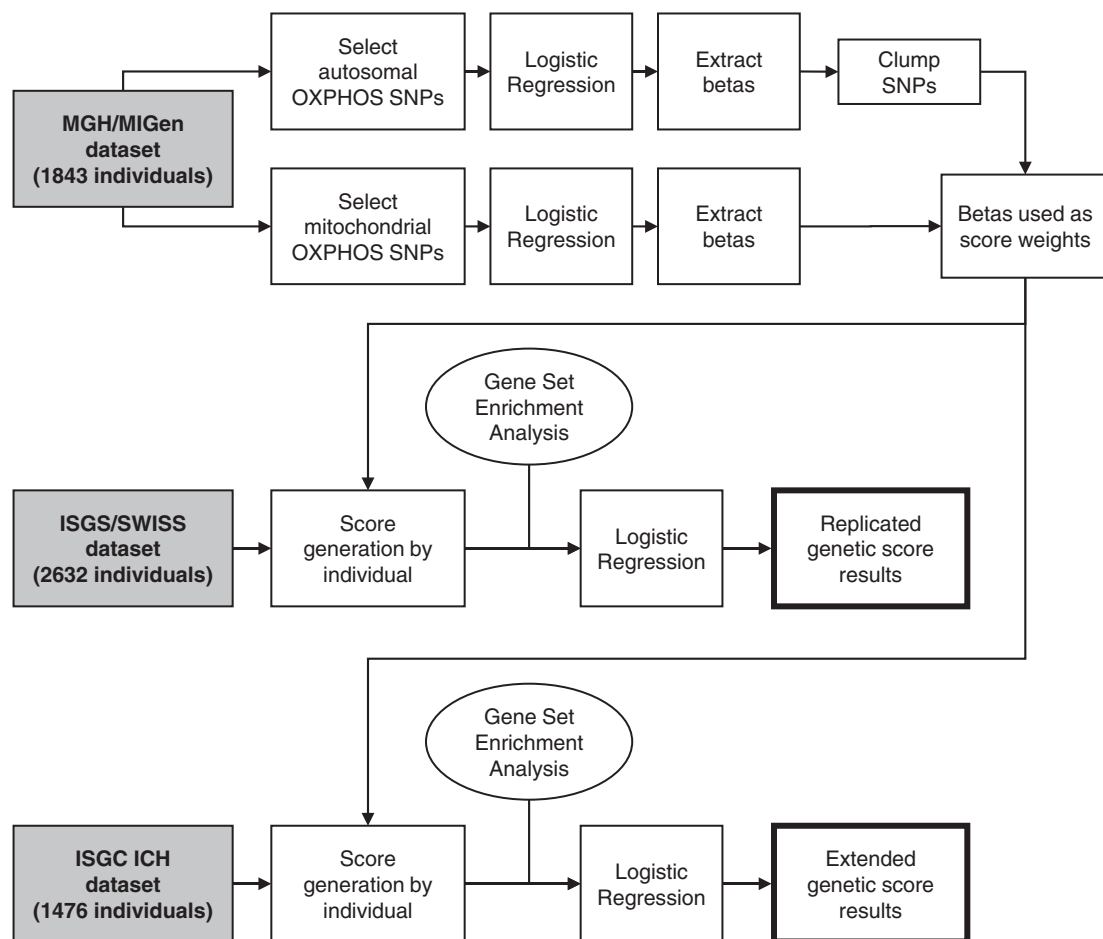


**Figure.** Flowchart describing the MGH/MIGen discovery, ISGS/SWISS validation, and ISGC ICH extension cohorts. ICH indicates intracerebral hemorrhage; ISGS, Ischemic Stroke Genetics Study; ISGC, International Stroke Genetics Consortium; MGH, Massachusetts General Hospital; OXPPOS, all structural proteins directly contributing to oxidative phosphorylation complex function; SNP, single nucleotide polymorphism; and SWISS, Siblings with Ischemic Stroke Study.

with the null hypothesis derived from random sampling of an equal number of variants of similar MAFs chosen from genes not within the OXPPOS pathway. Using this technique, the significance threshold for our GSEA was set at empirical  $P < 0.05$ .

### Genetic Score Generation in IS

Combined effects of all autosomal and mitochondrial OXPPOS SNPs were evaluated using a score-based method described previously<sup>4,12</sup> (Figure). Briefly, each OXPPOS SNP was tested for association with all-cause IS risk in the MGH/MIGen discovery case-control data set. The results of this analysis, expressed as a  $\beta$ -coefficient for the risk allele at each SNP, were then clumped according to linkage disequilibrium using the clump function in PLINK v1.07. Only the SNP with the highest significance value was retained in regions in which linkage disequilibrium was  $>0.6$  between SNPs. No additional pruning or thresholding was performed in an attempt to optimize the SNPs included in the genetic score. These  $\beta$ -coefficients were then applied to the corresponding OXPPOS SNPs in the ISGS/SWISS validation data set. All subsequent analyses in replication and extension were based on this single set of  $\beta$ -coefficients from the MGH/MIGen discovery cohort in association with all-cause IS (Table III in the online-only Data Supplement). After  $\beta$ -coefficient extraction, the MGH/MIGen discovery cohort was not included in any further analysis. A risk score was generated for each individual by summing the  $\beta$ -coefficients associated with each risk allele present in the individual. Informed by GSEA results, scores were developed for all OXPPOS complexes: complex I and complex IV. Because the risk score distributions failed testing for normality by Shapiro–Wilk, the score was divided into quintiles in an unsupervised fashion using the cut command in STATA v10.0 (<http://www.stata.com>) for association testing.

### Genetic Score Association Testing in IS

The IS risk score quintiles were used as the independent variable in an ordinal logistic regression model for IS risk, using age and sex as prespecified covariates. Results reported represent risk (as expressed by odds ratio [OR]) per unit increase in score quintile. SNPs that were present in the MGH/MIGen discovery cohort but were absent from the ISGS/SWISS validation cohort were dropped from the analysis ( $n=30$ ). Additional covariates of hypertension, diabetes mellitus, and atrial fibrillation were also tested. Results of genetic score testing in the replication and extension data sets represent independent tests. Therefore,  $P < 0.05$  in the replication and extension data sets is considered statistically significant. All regression analyses were performed using STATA v10.0.

### Extension of Genetic Score Analysis to ICH

The same  $\beta$ -coefficients of association with IS from the MGH/MIGen discovery cohort were applied to individuals within the ISGC ICH cohort, again resulting in a risk score for each individual. Risk score

quintiles were then used as the independent variable in a logistic regression for ICH risk, using age, sex, hypertension, and warfarin exposure as prespecified covariates. For ICH, scores were developed only for all OXPPOS and complex IV. Separate analyses were performed for deep and lobar ICH subtypes. Cerebellar and multicompartment ICH were included in the all ICH analysis but were dropped from deep and lobar analyses.

### Post Hoc Power Calculation

Power for discovery of association between individual variants within OXPPOS genes and IS was computed using the Genetic Power Calculator,<sup>19</sup> with calculated ORs of 1.10, 1.20, and 1.40 and MAF of 0.10, 0.20, and 0.30. For this analysis,  $\alpha$  was set at  $6 \times 10^{-5}$  (842 independent tests for autosomal and mitochondrial variants within OXPPOS genes).

Power to detect an association between the genetic risk score and stroke phenotypes was computed using the expected proportion of variance explained, assuming that the overall information content of the score would account for 0.5%, 1%, or 5% of variance between cases and controls. Power calculations were performed for IS, IS subtypes, ICH, and ICH deep, and lobar subgroups.

## Results

### Genotyping Quality Control and Imputation Results

Implementation of quality control and imputation methods left 1843 individuals and 707 autosomal SNPs in the MGH/MIGen cohort, 2632 individuals and 677 autosomal SNPs in the ISGS/SWISS cohort, and 1837 individuals and 707 autosomal SNPs in the ISGC ICH cohort (Figure 1); 135 mitochondrial SNPs were retained in all 3 cohorts after extraction and haplotype-based imputation (Appendix II in the online-only Data Supplement).

### GSEA in IS

GSEA was performed using the ISGS/SWISS cohort, testing the OXPPOS gene-set 100 000 times against randomly assigned gene-sets of equal size (Table 2). GSEA testing for the full OXPPOS gene-set and those within each respiratory complex demonstrated associations between IS and the full OXPPOS gene-set ( $P=0.012$ ), as well as OXPPOS complexes I and IV ( $P=0.024$  in both). Among IS subtypes, GSEA revealed significant association between small vessel (SV) stroke and OXPPOS complexes I and IV ( $P=0.008$  and  $P=0.005$ , respectively), although there was only a trend toward association between SV stroke and the full OXPPOS gene-set ( $P=0.091$ ).

**Table 2. Gene-Set Enrichment Analysis (P Values)**

	Cases/Controls	Full OXPPOS	Complex I	Complex II/III	Complex IV	Complex V
All ischemic stroke	1048/1384	0.012	0.024	$>0.20$	0.024	0.11
CE	241/1384	$>0.20$	$>0.20$	$>0.20$	$>0.20$	$>0.20$
LA	223/1384	$>0.20$	$>0.20$	$>0.20$	$>0.20$	$>0.20$
SV	197/1384	0.091	0.008	$>0.20$	0.005	$>0.20$
All ICH	928/548	$>0.20$	0.12	...	0.035	...
Lobar ICH	409/548	$>0.20$	$>0.20$	...	$>0.20$	...
Deep ICH	430/548	$>0.20$	0.16	...	0.009	...

Association between gene-sets and ischemic stroke (Ischemic Stroke Genetics Study/Siblings with Ischemic Stroke Study) and ICH (International Stroke Genetics Consortium ICH), with  $P$  values reported from 100 000 permutations against the null. CE indicates cardioembolic stroke; ICH, intracerebral hemorrhage; LA, large artery stroke; SV, small vessel stroke; OXPPOS, all structural proteins directly contributing to oxidative phosphorylation complex function; and ..., analysis not performed.

**Table 3. Genetic Score Analysis**

	Cases/Controls	Full OXPHOS		Complex I		Complex IV	
		OR (95% CI)	P Value	OR (95% CI)	P Value	OR (95% CI)	P Value
All ischemic stroke	1048/1384	1.17 (1.03–1.33)	0.008	1.06 (1.00–1.12)	0.050	1.05 (0.99–1.12)	0.075
SV only	197/1384	1.16 (1.04–1.29)	0.007	1.13 (1.01–1.26)	0.027	1.14 (1.02–1.27)	0.018
All ICH	928/548	...	...	...	...	1.08 (1.01–1.17)	0.039
Deep only	430/548	...	...	...	...	1.14 (1.03–1.25)	0.008

Genetic score analysis results in the Ischemic Stroke Genetics Study/Siblings with Ischemic Stroke Study validation cohort and International Stroke Genetics Consortium ICH extension cohort, performed only on gene-sets and subgroups with significant *P* values in gene-set enrichment analysis. ORs represent risk per unit increase in risk score quintile. CI indicates confidence interval; ICH, intracerebral hemorrhage; OR, odds ratio; OXPHOS, all structural proteins directly contributing to oxidative phosphorylation complex function; SV, small vessel stroke; and ..., analysis not performed. Nominal *P* values are reported for association with ischemic stroke and ICH in the validation and extension cohorts.

### GSEA in ICH

As with our IS analysis, GSEA was performed in the ISGC ICH cohort to determine whether OXPHOS gene-sets were enriched for association with ICH risk (Table 2). On the basis of our results from IS GSEA, only the full OXPHOS, complex I, and complex IV gene-sets were carried over for testing in ICH. An association was found between all ICH and complex IV ( $P=0.035$ ). After restricting cases to deep and lobar subgroups, deep ICH retained association with complex IV ( $P=0.008$ ).

### Genetic Score Analysis in IS

On the basis of GSEA results, only SNPs in the full OXPHOS gene-set as well as complexes I and IV were used to calculate genetic scores. Similarly, only all-cause IS and the SV subtype were carried forward for genetic score analysis (Table 3). Application of  $\beta$ -coefficient-based scores in the ISGS/SWISS cohort demonstrated associations between a score comprising the full OXPHOS gene-set and IS (OR, 1.17; 95% confidence interval [CI], 1.03–1.33). This full OXPHOS score was also associated with the SV stroke subtype (OR, 1.16; 95% CI, 1.04–1.29). Of note, these genetic score results were largely driven by autosomal variants, with results deviating <20% when mitochondrial variants were excluded (Table VI in the online-only Data Supplement).

In analysis of our complex I score, IS (OR, 1.06; 95% CI, 1.00–1.12) and the SV stroke subtype (OR, 1.13; 95% CI, 1.01–1.26) demonstrated significant association. For our complex IV score, there was a trending association for all-cause stroke and a significant association for SV stroke (OR, 1.14; 95% CI, 1.02–1.27).

Regression analyses for IS were performed with and without the inclusion of vascular risk factors as covariates in logistic regression (hypertension, diabetes mellitus, and atrial fibrillation). These regressors did not demonstrate significant association with the genetic scores and did not alter the results of the regression analysis ( $P=NS$ ; data not shown).

### Extension of Genetic Score Analysis to ICH

We constructed genetic scores in the ISGC ICH cohort based on  $\beta$ -coefficients from the MGH/MIGen IS cohort (Table 3). This analysis revealed association between a genetic score from complex IV genes and all ICH (OR, 1.08; 95% CI, 1.01–1.17;  $P=0.039$ ), as well as deep ICH (OR, 1.14; 95% CI, 1.03–1.25;  $P=0.008$ ).

### Post Hoc Power Calculation

Power calculations for discovery of individual OXPHOS genetic variants in association with IS revealed a maximum power of 73% to detect variants conferring an OR of 1.4 in association with IS risk at an MAF of 0.30 (Table III in the online-only Data Supplement). SNPs conferring lower OR and lower MAF substantially limited study power to detect individual variants, as did restriction of samples to the SV subtype. We performed power calculations for our genetic score analyses based on percentage of variance explained by the genetic score, ranging from 0.5% to 5%. The genetic score analysis was powered at 21%, to explain 0.5% of variance in IS risk for all-cause strokes and 3% to explain 0.5% of variance in the SV subtype. In application of this genetic score to ICH, power was 16%, to explain 0.5% of variance in all ICH and 8%, to explain 0.5% of variance in deep ICH (Table IV in the online-only Data Supplement). As a reference, percentages of variance explained in our logistic regression models incorporating genetic scores ranged from 0.5% to 1% in most analyses.

### Discussion

Our pathway-based analysis demonstrates that common genetic variants in OXPHOS genes are associated with risk of both IS and ICH. These associations are robust, having passed GSEA and replication in independent cohorts. Stratifying IS and ICH by subtype and OXPHOS genes by mitochondrial complex, we reveal associations for complexes I and IV in SV stroke and complex IV in deep ICH. These subanalyses retain significance, despite a substantial restriction in sample size and SNP counts.

Although ample evidence exists for rare mutations leading to severe OXPHOS dysfunction in a variety of familial mitochondrial syndromes with stroke phenotypes, our analysis provides evidence of a role for common genetic variants within OXPHOS in sporadic IS and ICH. These results contribute to a growing body of evidence linking OXPHOS genetic and functional variation to common neurological diseases, including Alzheimer disease, amyotrophic lateral sclerosis, and Parkinson disease, to name a few.<sup>20–23</sup>

Our subanalyses restricted to variants within complexes I and IV genes reveal additional parallels to rare mitochondrial syndromes. Mutations within complex I account for up to one third of the known respiratory chain diseases and

represent a major determinant of the redox state of the cell.<sup>24,25</sup> Complex IV is the final electron donor in the pathway, receiving electrons from cytochrome C and passing them to oxygen. Complex IV dysfunction, in addition to causing early life mitochondrial diseases such as Leigh disease and encephalomyopathies, has also been implicated in neurodegenerative diseases.<sup>20</sup> Although complex I is much larger than complex IV (50 versus 23 gene products), our demonstrated positive associations for both complexes suggest that statistical power alone did not determine our results, and the correlations with existing knowledge of mitochondrial disease supports a possible role for these complexes in sporadic human disease. Neither complex I nor complex IV dysfunction has effective treatments, although administration of cofactors has been reported to improve function in some instances.<sup>26</sup>

Both SV stroke and deep ICH result from disease of cerebral SVs and share common risk factors, such as diabetes mellitus and hypertension.<sup>27,28</sup> Our findings suggest a possible shared genetic contribution to SV pathobiology underlying SV stroke and deep ICH, which could be mediated through disruption in oxidative function at the tissue level or through modification of upstream systemic or endothelial risk factors shared by the 2 diseases. We previously reported an association between mitochondrial common variants and white matter hyperintensity volume,<sup>4</sup> a phenotype to which SV stroke and deep ICH have been linked.<sup>29,30</sup> These new data provide additional support for the role of energy metabolism in SV disease. However, given that OXPPOS dysfunction can result in numerous physiological derangements, including ATP depletion, reactive oxygen species generation, defects in cell signaling, and alteration in apoptotic thresholds, our demonstrated associations cannot directly inform the underlying pathobiology of this SV link. Functional studies to identify the mechanisms of bioenergetic dysfunction will be needed to build on these results.

APOE allele status has been demonstrated to affect the risk and severity of lobar ICH, presumably attributable to a strong relationship between cerebral amyloid angiopathy and the lobar ICH subtype.<sup>11,13</sup> The present study suggests a relationship between OXPPOS variants and deep ICH only, contributing to growing evidence that deep and lobar ICH represent genetically distinct entities. Genetic approaches seem to be useful tools to explore the differences between these ICH subtypes and hopefully can lead to a more comprehensive understanding of the pathogenesis of these similar but unique disease subtypes.

Limitations render our results preliminary. The magnitude of effect sizes for OXPPOS genetic scores in stroke risk in our analyses are small but are inline with the results from other GWAS efforts in ischemic and hemorrhagic stroke.<sup>2-4,8,11,13</sup> Our GSEA did not find associations for the large artery or cardioembolic stroke subtypes in IS or the lobar subtype in ICH. Given our power calculations, it is possible that the restriction in sample size for subtype-stratified analyses led to a false-negative for these subtypes. Therefore, we cannot definitively demonstrate that the effect of OXPPOS genetic variants on ischemic or hemorrhagic stroke is isolated to SV ischemic or deep ICH subtypes. Many subjects in the MGH/MiGen and ISGS/SWISS data sets were used in previous study of mitochondrial variants in IS, although the method of analysis

differed between these studies.<sup>4</sup> These data sets theoretically could be particularly enriched with OXPPOS associations, although the positive extension to the ISGC ICH cohort would not be predicted if this were the case.

Genetic score analysis, although effective in aggregating signals to detect association, cannot identify individual causative variants. As a result, we are unable to determine the particular genetic loci conferring risk in the present study. GWAS platform-based SNPs were used in this analysis, which are not highly enriched for functional variants likely to cause missense, nonsense, or splice-site mutations. It is possible that other common or rare genetic variants in the OXPPOS pathway lie in linkage disequilibrium with our included variants, exerting a more substantial effect in affected individuals. Given the small aggregate effect sizes of the genetic scores in our analysis, prohibitively large sample sizes would be required to achieve sufficient power to detect individual OXPPOS variants. The significance thresholds in the current study were set according to established techniques in GSEA and genetic score analysis and can be considered robust because of the use of permutation in the case of GSEA and the use of separate discovery and replication cohorts in the case of the genetic score analysis. Because the majority of genes encoding OXPPOS proteins are autosomal, we cannot determine whether the low-risk contribution ( $\leq 20\%$ ) of mitochondrial variants to the risk scores for IS and ICH in our analysis is attributable to an imbalance in SNP contributions to the genetic score or a true difference in risk proportion. Finally, we cannot determine whether the involvement of the OXPPOS pathway in IS and ICH is mediated at the brain tissue level or possibly through modification of systemic vascular or metabolic risk factors. Follow-up analyses will be required to address OXPPOS function in different tissue types.

## Conclusions

Through a pathway-based analysis, we have demonstrated that genetic variation within genes involved in the OXPPOS apparatus associates with IS risk, particularly the SV stroke subtype. Extension to ICH reveals retained association with OXPPOS complex IV in deep ICH. Further studies will be necessary to clarify the functional impact of these variants on OXPPOS function.

## Acknowledgments

This work used samples and clinical data from the National Institutes of Neurological Disorders and Stroke Human Genetics Resource Center DNA and Cell Line Repository (<http://ccr.coriell.org/ninds>). This study used the high-performance computational capabilities of the Biowulf Linux cluster at the National Institutes of Health (NIH), Bethesda, MD (<http://biowulf.nih.gov>). The project described was supported in part by a grant from the National Institute of Neurological Disorders and Stroke (NINDS) and National Institute on Minority Health and Health Disparities (NS U54NS057405). The content is solely the responsibility of the authors and does not necessarily represent the official views of NINDS or NIH.

C. Anderson (coleader), A. Biffi (coleader), and J. Rosand were responsible for manuscript preparation. Data acquisition was performed by C. Anderson, N. Rost, A. Ayres, K. Schwab, A. Viswanathan, M. Nalls, W. Devan, V. Valant, B. Hansen, and A. Biffi. Manuscript revision was completed by N. Rost, M. Nalls, O. Ross, R. Saxena, J. Meschia,

W. Devan, V. Valant, J. Rosand, B. Worrall, T. Brott, D. Brown, B. Hansen, J. Broderick, B. Norrving, A. Viswanathan, S. Silliman, D. Tirschwell, A. Lindgren, A. Slowik, R. Schmidt, M. Selim, J. Roquer, J. Montaner, A. Singleton, S. Greenberg, C. Kidwell, D. Woo, C. Anderson, A. Biffi, and M. Nalls conducted data analysis. Study management was performed by J. Rosand, K. Furie, J. Goldstein, J. Meschia, A. Singleton, T. Brott, B. Worrall, O. Ross, D. Brown, J. Broderick, B. Norrving, A. Viswanathan, S. Silliman, D. Tirschwell, A. Lindgren, A. Slowik, R. Schmidt, M. Selim, J. Roquer, J. Montaner, A. Singleton, S. Greenberg, C. Kidwell, and D. Woo.

### Sources of Funding

Massachusetts General Hospital/MiGen: These studies were funded by the American Heart Association/Bugher Foundation Centers for Stroke Prevention Research (0775010 N), the National Institutes of Health (NIH)—National Institute for Neurological Disorders and Stroke (NINDS; R01 NS059727, U01 NS069208), The Keane Genetics Fund, and the Deane Institute for Integrative Research in Atrial Fibrillation and Stroke. The MiGen study was funded by the US NIH and National Heart, Lung, and Blood Institute STAMPEED genomics research program (R01 HL087676) and a grant from the National Center for Research Resources. The Broad Institute Center for Genotyping and Analysis is supported by grant U54 RR020278 from the National Center for Research resources. C.D.A., A.B., and N.S.R. were supported in part by the American Heart Association/Bugher Foundation Centers for Stroke Prevention Research, and C.D.A. was supported by the American Brain Foundation.

Ischemic Stroke Genetics Study/Siblings with Ischemic Stroke Study: These studies were funded by NIH-NINDS (R01 NS42733, R01 NS39987), the Intramural Research Program of NIH-National Institute on Aging (NIA; Z01 AG000954-06), and by the Marriott Disease Risk and Regenerative Medicine Initiative Award in Individualized Medicine and the Marriott Mitochondrial Fund. The inclusion of BLSA samples was supported in part by the Intramural Research Program of NIH-NIA (Z01 AG000015-50). O.A.R. was supported by the American Heart Association, James and Esther King Biomedical Research Program, the Florida Department of Health, and the Myron and Jane Hanley Award in Stroke Research.

International Stroke Genetics Consortium: The Differences in the Imaging of Primary Hemorrhage based on Ethnicity or Race (DECIPHER) project was supported by Award Number U54NS057405 from the NIH-NINDS and National Institute on Minority Health and Health Disparities (NIMHD) (U54NS057405). The content is solely the responsibility of the authors and does not necessarily represent the official views of the National Institute of Neurological Disorders and Stroke or the National Institutes of Health (DECIPHER). The Genetic and Environmental Risk Factors for Hemorrhagic Stroke (GERFHS) study was supported by NIH-NINDS (NS36695 and NS30678), and by the Greater Cincinnati Foundation Grant (Cincinnati Control Cohort). The Massachusetts General Hospital Intracerebral Hemorrhage Stroke Genome-Wide Association study was funded by NIH-NINDS (K23NS042695, 5K23NS059774, R01NS059727, and 5R01NS042147), the Keane Stroke Genetics Research Fund, the Edward and Maybeth Sonn Research Fund, by the University of Michigan General Clinical Research Center (M01 RR000042), and by a grant from the National Center for Research Resources. The Hospital del Mar ICH (HM-ICH) study was funded by the Instituto de Salud Carlos III, Spanish Research Networks Red HERACLES (RD06/009) FEDER. The Jagiellonian University Hemorrhagic Stroke Study (JUHSS) was supported by a grant funded by the Polish Ministry of Education (NN402083934). The Lund Stroke Register (LSR) was funded by Lund University, Region Skåne, King Gustaf V's and Queen Victoria's Foundation, and the Swedish Medical Research Council (K2010-61X-20378-04-3). Biobank services and genotyping were done at Region Skåne Competence Center (RSKC Malmö), Skåne University Hospital, Malmö, Sweden. Controls from the Medical University of Graz ICH (MUG-ICH) study were from the Austrian Stroke Prevention Study, which is a population-based study funded by the Austrian Science Fund grant numbers P20545-P05 and P13180; the Medical University of Graz supports the databank of the Austrian Stroke Prevention Study.

### Disclosures

None.

### References

- Flossmann E, Schulz UG, Rothwell PM. Systematic review of methods and results of studies of the genetic epidemiology of ischemic stroke. *Stroke*. 2004;35:212–227.
- Meschia JF. Advances in genetics 2010. *Stroke*. 2011;42:285–287.
- Bellenguez C, Bevan S, Gschwendtner A, Spencer CC, Burgess AI, Pirinen M, et al. Genome-wide association study identifies a variant in *hdac9* associated with large vessel ischemic stroke. *Nat Genet*. 2012;44:328–333.
- Anderson CD, Biffi A, Rahman R, Ross OA, Jagiella JM, Kissela B, et al; International Stroke Genetics Consortium. Common mitochondrial sequence variants in ischemic stroke. *Ann Neurol*. 2011;69:471–480.
- Wagner BK, Kitami T, Gilbert TJ, Peck D, Ramanathan A, Schreiber SL, et al. Large-scale chemical dissection of mitochondrial function. *Nat Biotechnol*. 2008;26:343–351.
- DiMauro S, Schon EA. Mitochondrial disorders in the nervous system. *Annu Rev Neurosci*. 2008;31:91–123.
- Nicholls DG. Oxidative stress and energy crises in neuronal dysfunction. *Ann NY Acad Sci*. 2008;1147:53–60.
- Anderson CD, Biffi A, Rost NS, Cortellini L, Furie KL, Rosand J. Chromosome 9p21 in ischemic stroke: population structure and meta-analysis. *Stroke*. 2010;41:1123–1131.
- Meschia JF, Brott TG, Brown RD Jr, Crook RJ, Frankel M, Hardy J, et al; Ischemic Stroke Genetics Study. The Ischemic Stroke Genetics Study (ISGS) Protocol. *BMC Neurol*. 2003;3:4.
- Meschia JF, Brown RD Jr, Brott TG, Chukwudelunzu FE, Hardy J, Rich SS. The Siblings With Ischemic Stroke Study (SWISS) protocol. *BMC Med Genet*. 2002;3:1.
- Biffi A, Anderson CD, Jagiella JM, Schmidt H, Kissela B, Hansen BM, et al; International Stroke Genetics Consortium. APOE genotype and extent of bleeding and outcome in lobar intracerebral haemorrhage: a genetic association study. *Lancet Neurol*. 2011;10:702–709.
- Kathiresan S, Willer CJ, Peloso GM, Demissie S, Musunuru K, Schadt EE, et al. Common variants at 30 loci contribute to polygenic dyslipidemia. *Nat Genet*. 2009;41:56–65.
- Biffi A, Sonni A, Anderson CD, Kissela B, Jagiella JM, Schmidt H, et al; International Stroke Genetics Consortium. Variants at APOE influence risk of deep and lobar intracerebral hemorrhage. *Ann Neurol*. 2010;68:934–943.
- Saxena R, de Bakker PI, Singer K, Mootha V, Burt N, Hirschhorn JN, et al. Comprehensive association testing of common mitochondrial DNA variation in metabolic disease. *Am J Hum Genet*. 2006;79:54–61.
- Turner S, Armstrong LL, Bradford Y, Carlson CS, Crawford DC, Crenshaw AT, et al. Quality control procedures for genome-wide association studies. *Curr Protoc Hum Genet*. 2011; Unit 1.19.
- Biffi A, Anderson CD, Nalls MA, Rahman R, Sonni A, Cortellini L, et al. Principal-component analysis for assessment of population stratification in mitochondrial medical genetics. *Am J Hum Genet*. 2010;86:904–917.
- Subramanian A, Tamayo P, Mootha VK, Mukherjee S, Ebert BL, Gillette MA, et al. Gene set enrichment analysis: A knowledge-based approach for interpreting genome-wide expression profiles. *Proc Natl Acad Sci USA*. 2005;102:15545–15550.
- Wang K, Li M, Bucan M. Pathway-based approaches for analysis of genomewide association studies. *Am J Hum Genet*. 2007;81:1278–1283.
- Purcell S, Cherny SS, Sham PC. Genetic power calculator: design of linkage and association genetic mapping studies of complex traits. *Bioinformatics*. 2003;19:149–150.
- Müller WE, Eckert A, Kurz C, Eckert GP, Leuner K. Mitochondrial dysfunction: common final pathway in brain aging and Alzheimer's disease—therapeutic aspects. *Mol Neurobiol*. 2010;41:159–171.
- Duan W, Li X, Shi J, Guo Y, Li Z, Li C. Mutant TAR DNA-binding protein-43 induces oxidative injury in motor neuron-like cell. *Neuroscience*. 2010;169:1621–1629.
- López-Gallardo E, Iceta R, Iglesias E, Montoya J, Ruiz-Pesini E. OXPHOS toxicogenomics and Parkinson's disease. *Mutat Res*. 2011;728:98–106.
- Coskun P, Wyrembak J, Schriener SE, Chen HW, Marciniack C, Laferla F, et al. A mitochondrial etiology of Alzheimer and Parkinson disease. *Biochim Biophys Acta*. 2012;1820:553–564.



24. Rich PR, Maréchal A. The mitochondrial respiratory chain. *Essays Biochem.* 2010;47:1–23.
25. Stefanatos R, Sanz A. Mitochondrial complex I: a central regulator of the aging process. *Cell Cycle.* 2011;10:1528–1532.
26. Lagoa R, Graziani I, Lopez-Sanchez C, Garcia-Martinez V, Gutierrez-Merino C. Complex I and cytochrome c are molecular targets of flavonoids that inhibit hydrogen peroxide production by mitochondria. *Biochim Biophys Acta.* 2011;1807:1562–1572.
27. Putaala J, Liebkind R, Gordin D, Thorn LM, Haapaniemi E, Forsblom C, et al. Diabetes mellitus and ischemic stroke in the young: clinical features and long-term prognosis. *Neurology.* 2011;76:1831–1837.
28. Bokura H, Saika R, Yamaguchi T, Nagai A, Oguro H, Kobayashi S, et al. Microbleeds are associated with subsequent hemorrhagic and ischemic stroke in healthy elderly individuals. *Stroke.* 2011;42:1867–1871.
29. Rost NS, Rahman RM, Biffi A, Smith EE, Kanakis A, Fitzpatrick K, et al. White matter hyperintensity volume is increased in small vessel stroke subtypes. *Neurology.* 2010;75:1670–1677.
30. Yamada S, Saiki M, Satow T, Fukuda A, Ito M, Minami S, et al. Periventricular and deep white matter leukoaraiosis have a closer association with cerebral microbleeds than age. *Eur J Neurol.* 2012;19:98–104.

SUPPLEMENTARY DATA

Common Variants within Oxidative Phosphorylation Genes Influence Risk of Ischemic Stroke and Intracerebral Hemorrhage

CD Anderson et al.

## Table of Contents:

1. Supplementary Appendix I: Mitochondrial DNA genotyping and imputation methods
2. Supplementary Appendix II: Genotyping quality control and imputation results
3. Supplementary Table S1: Autosomal oxidative phosphorylation genes, locations, and functional annotations
4. Supplementary Table S2: Mitochondrial oxidative phosphorylation SNPs, platforms, associated genes, locations, and functional annotations
5. Supplementary Table S3: Beta associations for risk of all-cause ischemic stroke in the MGH/MIGen discovery cohort for genotyped autosomal and mitochondrial variants
6. Supplementary Table S4: Statistical power to discover association between individual OXPHOS genetic variants and ischemic stroke
7. Supplementary Table S5: Statistical power to discover association between OXPHOS genetic risk score and ischemic stroke and intracerebral hemorrhage
8. Supplementary Table S6: Change in odds ratio point estimates and p-values from Table 3 with omission of mitochondrial variants from the genetic score

## Supplementary Appendix I. Mitochondrial DNA genotyping and imputation methods

For genotype ascertainment and quality control of mitochondrial SNPs, raw intensity files were inspected for all mtDNA variants. Direct inspection was employed by two investigators (C.D.A. and A.B.) to confirm genotyping quality and genotype assignment. For mitochondrial variants, missingness by individual was restricted to no more than 1%, in addition to the standard quality control cutoffs employed for autosomal variants. Tests of differential missingness by case/control status were employed to ensure that no mitochondrial variant was preferentially missing in either cases or controls in the discovery, replication, and extension cohorts.

According to previously published methods<sup>1</sup>, we aligned all human mtDNA coding-region sequences from GenBank (719 sequences) and 536 sequences from Mitokor; we identified a total of 3,240 variant sites. Of note, we excluded ~0.8 kb of the hypervariable mtDNA D-loop promoter region from the study, since this region is best addressed by direct resequencing in case-control samples because of its high mutation rate. The combined dataset arising from these two sources was then used as model for haplotype-based imputation using a previously described approach<sup>2</sup>. Briefly, available genotypes from reference datasets mentioned above were used to construct haplotypes using the linear discriminant function analysis in the R v 2.10.0 statistical package. The accuracy of haplogroup prediction was determined via a bootstrap cross-validation approach. For each of 1000 replicates, a bootstrap sample of sequences was chosen to form the prediction model, and the unsampled sequences had their haplogroups predicted. The prediction accuracy was then determined simply as the proportions of sequences whose haplogroups were correctly predicted. In line with previously reported results, 95% of all crossvalidation replicates had a prediction accuracy of > 98.5%. Missing genotypes in the research datasets were finally imputed using the --hap-impute routine in PLINK v1.07, and subsequently filtered to include only SNPs within OXPHOS genes.

### References for Supplementary Appendix I:

1. Saxena R, de Bakker PI, Singer K, Mootha V, Burt N, Hirschhorn JN, et al. Comprehensive association testing of common mitochondrial DNA variation in metabolic disease. *American journal of human genetics*. 2006;79:54-61.
2. Biffi A, Anderson CD, Nalls MA, Rahman R, Sonni A, Cortellini L, et al. Principal-component analysis for assessment of population stratification in mitochondrial medical genetics. *American journal of human genetics*. 2010;86:904-917.

## Supplementary Appendix II. Genotyping quality control and imputation results

After implementation of quality control measures and imputation to HapMap Phase 3, 1843 individuals remained in the MGH cohort, with genotypes at 850,489 autosomal SNPs. After restricting the dataset to SNPs within the designated OXPHOS regions, 707 autosomal SNPs were left for final analysis. In the ISGS/SWISS validation cohort, similar quality control and imputation processes resulted in 2632 individuals with genotypes at 764,004 autosomal SNPs. Restriction to OXPHOS gene regions left 677 autosomal SNPs for analysis. Fewer than 10% of these SNPs had  $MAF < 0.05$ .

For all individuals meeting quality control criteria, extraction and haplotype-based imputation resulted in a total of 144 mitochondrial SNPs in the MGH/MIGen and ISGS/SWISS datasets, with 135 mitochondrial SNPs satisfying quality control criteria in both cohorts.

In the ISGC ICH cohort, quality control measures and HapMap Phase 3 imputation left 1837 individuals and 1,484,915 SNPs. Restriction to OXPHOS gene regions left 707 autosomal SNPs, and haplotype-based imputation left 135 mitochondrial SNPs for analysis.

Supplementary Table S1. Autosomal Oxidative Phosphorylation Genes, Locations, and Functional Annotations

CHR	START	END	GENE	ENTREZ	FUNCTION
8	95908041	96087923	C8orf38	137682	OXPHOS biogenesis/regulation Complex I
17	46970127	46973233	ATP5G1	516	OXPHOS Complex V
22	30163358	30166402	UCRC	29796	OXPHOS Complex III
19	19626540	19646885	NDUFA13	51079	OXPHOS Complex I
8	125551343	125562226	NDUFB9	4715	OXPHOS Complex I
4	140188034	140223705	NDUFC1	4717	OXPHOS Complex I
16	31439055	31439731	COX6A2	1339	OXPHOS Complex IV
19	36139155	36149683	COX6B1	1340	OXPHOS Complex IV
5	85913721	85916779	COX7C	1350	OXPHOS Complex IV
19	36641824	36643771	COX7A1	1346	OXPHOS Complex IV
21	27088815	27107984	ATP5J	522	OXPHOS Complex V
7	99046098	99063954	ATP5J2	9551	OXPHOS Complex V
7	140390577	140422590	NDUFB2	4708	OXPHOS Complex I
12	4758283	4796397	NDUFA9	4704	OXPHOS Complex I
1	39491990	39500308	NDUFS5	4725	OXPHOS Complex I
11	67798094	67804114	NDUFS8	4728	OXPHOS Complex I
1	161166894	161184185	NDUFS2	4720	OXPHOS Complex I
5	132202252	132203723	UQCRQ	27089	OXPHOS Complex III
6	97337189	97345757	NDUFAF4	29078	OXPHOS biogenesis/regulation Complex I
7	10971578	10979883	NDUFA4	4697	OXPHOS Complex I
11	47600632	47606113	NDUFS3	4722	OXPHOS Complex I
3	48636435	48648409	UQCRC1	7384	OXPHOS Complex III
5	52856463	52979168	NDUFS4	4724	OXPHOS Complex I
10	7830092	7849778	ATP5C1	509	OXPHOS Complex V
14	32030591	32330399	NUBPL	80224	OXPHOS biogenesis/regulation Complex I
1	161284047	161332984	SDHC	6391	OXPHOS Complex II
2	240831867	240964819	NDUFA10	4705	OXPHOS Complex I
18	9102628	9134343	NDUFV2	4729	OXPHOS Complex I
9	124906337	124922098	NDUFA8	4702	OXPHOS Complex I
5	1801514	1816719	NDUFS6	4726	OXPHOS Complex I
14	50779047	50802276	ATP5S	27109	OXPHOS Complex V
19	29698167	29704136	UQCRC1	7386	OXPHOS Complex III
15	41679547	41694658	NDUFAF1	51103	OXPHOS biogenesis/regulation Complex I

Supplementary Table S1 (continued)

CHR	START	END	GENE	ENTREZ	FUNCTION	
	5	218356	256815	SDHA	6389	OXPPOS Complex II
	12	120875904	120878532	COX6A1	1337	OXPPOS Complex IV
	9	32552997	32573160	NDUFB6	4712	OXPPOS Complex I
	16	21963981	21994981	UQCRC2	7385	OXPPOS Complex III
	1	47098409	47134099	ATPAF1	64756	OXPPOS biogenesis/regulation Complex V
	17	73034955	73043074	ATP5H	10476	OXPPOS Complex V
	6	75947391	75966492	COX7A2	1347	OXPPOS Complex IV
	17	17918373	17942523	ATPAF2	91647	OXPPOS biogenesis/regulation Complex V
	1	17345217	17380665	SDHB	6390	OXPPOS Complex II
	2	201936156	201950473	NDUFB3	4709	OXPPOS Complex I
	3	119373360	119396301	COX17	10063	OXPPOS biogenesis/regulation Complex IV
	2	206986149	207024327	NDUFS1	4719	OXPPOS Complex I
	19	1383883	1395587	NDUFS7	374291	OXPPOS Complex I
	17	13972846	14111994	COX10	1352	OXPPOS biogenesis/regulation Complex IV
	4	666225	668127	ATP5I	521	OXPPOS Complex V
	18	43664110	43684300	ATP5A1	498	OXPPOS Complex V
	3	120315156	120321347	NDUFB4	4710	OXPPOS Complex I
	19	54606036	54614898	NDUFA3	4696	OXPPOS Complex I
	2	98262503	98264846	COX5B	1329	OXPPOS Complex IV
	4	73921797	73935472	COX18	285521	OXPPOS biogenesis/regulation Complex IV
	19	14676892	14682886	NDUFB7	4713	OXPPOS Complex I
	2	176040986	176049335	ATP5G3	518	OXPPOS Complex V
	11	77779403	77791265	NDUFC2	4718	OXPPOS Complex I
	1	111991486	112005395	ATP5F1	515	OXPPOS Complex V
	10	102283497	102289757	NDUFB8	4714	OXPPOS Complex I
	5	159685260	159685595	LOC727947	727947	OXPPOS Complex III
	11	111957622	111966517	SDHD	6392	OXPPOS Complex II
	16	2009519	2011976	NDUFB10	4716	OXPPOS Complex I
	8	100890372	100905895	COX6C	1345	OXPPOS Complex IV
	17	47481414	47492246	PHB	5245	OXPPOS stress response
	8	145149960	145152427	CYC1	1537	OXPPOS Complex III
	19	8376234	8386280	NDUFA7	4701	OXPPOS Complex I
	19	5894686	5904025	NDUFA11	126328	OXPPOS Complex I
	16	23592323	23607677	NDUFAB1	4706	OXPPOS Complex I

Supplementary Table S1 (continued)

CHR	START	END	GENE	ENTREZ	FUNCTION
21	35275757	35288284	ATP5O	539	OXPHOS Complex V
3	179322478	179345435	NDUFB5	4711	OXPHOS Complex I
21	44299754	44427677	NDUFV3	4731	OXPHOS Complex I
22	42481529	42486888	NDUFA6	4700	OXPHOS Complex I
9	136218610	136223552	SURF1	6834	OXPHOS biogenesis/regulation Complex IV
20	30225691	30232809	COX4I2	84701	OXPHOS Complex IV
17	53029267	53046054	COX11	1353	OXPHOS biogenesis/regulation Complex IV
11	63742079	63744014	COX8A	1351	OXPHOS Complex IV
11	67374323	67380012	NDUFV1	4723	OXPHOS Complex I
7	123177051	123198309	NDUFA5	4698	OXPHOS Complex I
5	140018325	140027370	NDUFA2	4695	OXPHOS Complex I
19	1597180	1605431	UQCR	10975	OXPHOS Complex III
10	101471601	101491866	COX15	1355	OXPHOS biogenesis/regulation Complex IV
1	46769303	46782448	UQCRH	7388	OXPHOS Complex III
12	54058950	54071182	ATP5G2	517	OXPHOS Complex V
16	85833290	85840608	COX4I1	1327	OXPHOS Complex IV
7	25159710	25164980	CYCS	54205	OXPHOS Complex III
19	1241749	1244823	ATP5D	513	OXPHOS Complex V
12	95365109	95397511	NDUFA12	55967	OXPHOS Complex I
19	11616745	11639987	ECSIT	51295	OXPHOS biogenesis/regulation Complex I
15	75212132	75230509	COX5A	9377	OXPHOS Complex IV
5	60240956	60448853	NDUFAF2	91942	OXPHOS biogenesis/regulation Complex I
19	55861070	55866182	COX6B2	125965	OXPHOS Complex IV
12	57031963	57039852	ATP5B	506	OXPHOS Complex V
8	97238148	97247862	UQCRB	156467	OXPHOS Complex III
23	77154935	77162870	COX7B	1349	OXPHOS Complex IV
23	119005450	119010625	NDUFA1	4694	OXPHOS Complex I
23	47001615	47004903	NDUFB11	54539	OXPHOS Complex I

CHR = chromosome, ENTREZ = Entrez Gene ID, OXHOS = oxidative phosphorylation



Supplementary Table S2. Mitochondrial Oxidative Phosphorylation SNPs, Platforms, Associated Genes, Locations, and Functional Annotations

SNP	PLATFORM	START	END	GENE	ENTREZ	FUNCTION
mt150	DIRECT	1	579	D-Loop	N/A	Mitochondrial function
mt217	ILLUMINA610	1	579	D-Loop	N/A	Mitochondrial function
mt228	ILLUMINA610	1	579	D-Loop	N/A	Mitochondrial function
mt247	ILLUMINA610	1	579	D-Loop	N/A	Mitochondrial function
mt295	ILLUMINA610	1	579	D-Loop	N/A	Mitochondrial function
mt458	ILLUMINA610	1	579	D-Loop	N/A	Mitochondrial function
mt464	ILLUMINA610	1	579	D-Loop	N/A	Mitochondrial function
mt479	ILLUMINA610	1	579	D-Loop	N/A	Mitochondrial function
mt491	ILLUMINA610	1	579	D-Loop	N/A	Mitochondrial function
mt709	DIRECT	651	1604	12S rRNA	N/A	Mitochondrial function
mt750	DIRECT	651	1604	12S rRNA	N/A	Mitochondrial function
mt750	ILLUMINA610	651	1604	12S rRNA	N/A	Mitochondrial function
mt827	ILLUMINA610	651	1604	12S rRNA	N/A	Mitochondrial function
mt930	DIRECT	651	1604	12S rRNA	N/A	Mitochondrial function
mt1048	ILLUMINA610	651	1604	12S rRNA	N/A	Mitochondrial function
mt1189	DIRECT	651	1604	12S rRNA	N/A	Mitochondrial function
mt1189	ILLUMINA610	651	1604	12S rRNA	N/A	Mitochondrial function
mt1243	DIRECT	651	1604	12S rRNA	N/A	Mitochondrial function
mt1438	ILLUMINA610	651	1604	12S rRNA	N/A	Mitochondrial function
mt1719	DIRECT	1674	3231	16S rRNA	N/A	Mitochondrial function
mt1719	ILLUMINA610	1674	3231	16S rRNA	N/A	Mitochondrial function
mt1736	ILLUMINA610	1674	3231	16S rRNA	N/A	Mitochondrial function
mt1811	DIRECT	1674	3231	16S rRNA	N/A	Mitochondrial function
mt1888	DIRECT	1674	3231	16S rRNA	N/A	Mitochondrial function
mt2160	ILLUMINA610	1674	3231	16S rRNA	N/A	Mitochondrial function
mt2485	ILLUMINA610	1674	3231	16S rRNA	N/A	Mitochondrial function
mt2706	DIRECT	1674	3231	16S rRNA	N/A	Mitochondrial function
mt2706	ILLUMINA610	1674	3231	16S rRNA	N/A	Mitochondrial function
mt2789	ILLUMINA610	1674	3231	16S rRNA	N/A	Mitochondrial function
mt2885	ILLUMINA610	1674	3231	16S rRNA	N/A	Mitochondrial function
mt3010	DIRECT	1674	3231	16S rRNA	N/A	Mitochondrial function
mt3010	ILLUMINA610	1674	3231	16S rRNA	N/A	Mitochondrial function
mt3197	DIRECT	1674	3231	16S rRNA	N/A	Mitochondrial function

Supplementary Table S2 (continued)

SNP	PLATFORM	START	END	GENE	ENTREZ	FUNCTION
mt3197	ILLUMINA610	1674	3231	16S rRNA	N/A	Mitochondrial function
mt4336	DIRECT	4265	4333	tRNA-Ile	N/A	Mitochondrial function
mt4336	ILLUMINA610	4265	4333	tRNA-Ile	N/A	Mitochondrial function
mt5656	DIRECT	5589	5731	tRNA-Ala	N/A	Mitochondrial function
mt5773	ILLUMINA610	5763	5828	tRNA-Cys	N/A	Mitochondrial function
mt7476	DIRECT	7448	7518	tRNA-Ser	N/A	Mitochondrial function
mt8278	ILLUMINA610	8272	8366	tRNA-Lys	N/A	Mitochondrial function
mt10034	DIRECT	9993	10060	tRNA-Gly	N/A	Mitochondrial function
mt10034	ILLUMINA610	9993	10060	tRNA-Gly	N/A	Mitochondrial function
mt10045	ILLUMINA610	9993	10060	tRNA-Gly	N/A	Mitochondrial function
mt12308	DIRECT	12268	12338	tRNA-Ser	N/A	Mitochondrial function
mt12309	ILLUMINA610	12268	12338	tRNA-Ser	N/A	Mitochondrial function
mt14687	DIRECT	14676	14744	tRNA-Glu	N/A	Mitochondrial function
mt15904	DIRECT	15890	15995	tRNA-Thr	N/A	Mitochondrial function
mt15904	ILLUMINA610	15890	15995	tRNA-Thr	N/A	Mitochondrial function
mt15924	DIRECT	15890	15995	tRNA-Thr	N/A	Mitochondrial function
mt15924	ILLUMINA610	15890	15995	tRNA-Thr	N/A	Mitochondrial function
mt15928	DIRECT	15890	15995	tRNA-Thr	N/A	Mitochondrial function
mt15928	ILLUMINA610	15890	15995	tRNA-Thr	N/A	Mitochondrial function
mt15931	ILLUMINA610	15890	15995	tRNA-Thr	N/A	Mitochondrial function
mt3348	ILLUMINA610	3309	4264	ND1	4535	OXPPOS Complex I
mt3394	DIRECT	3309	4264	ND1	4535	OXPPOS Complex I
mt3394	ILLUMINA610	3309	4264	ND1	4535	OXPPOS Complex I
mt3480	DIRECT	3309	4264	ND1	4535	OXPPOS Complex I
mt3480	ILLUMINA610	3309	4264	ND1	4535	OXPPOS Complex I
mt3505	DIRECT	3309	4264	ND1	4535	OXPPOS Complex I
mt3594	ILLUMINA610	3309	4264	ND1	4535	OXPPOS Complex I
mt3666	ILLUMINA610	3309	4264	ND1	4535	OXPPOS Complex I
mt3721	ILLUMINA610	3309	4264	ND1	4535	OXPPOS Complex I
mt3915	DIRECT	3309	4264	ND1	4535	OXPPOS Complex I
mt3915	ILLUMINA610	3309	4264	ND1	4535	OXPPOS Complex I
mt3918	ILLUMINA610	3309	4264	ND1	4535	OXPPOS Complex I

Supplementary Table S2 (continued)

SNP	PLATFORM	START	END	GENE	ENTREZ	FUNCTION
mt3971	ILLUMINA610	3309	4264	ND1	4535	OXPHOS Complex I
mt3993	ILLUMINA610	3309	4264	ND1	4535	OXPHOS Complex I
mt4025	ILLUMINA610	3309	4264	ND1	4535	OXPHOS Complex I
mt4216	DIRECT	3309	4264	ND1	4535	OXPHOS Complex I
mt4529	DIRECT	4472	5513	ND2	4536	OXPHOS Complex I
mt4580	DIRECT	4472	5513	ND2	4536	OXPHOS Complex I
mt4769	ILLUMINA610	4472	5513	ND2	4536	OXPHOS Complex I
mt4793	DIRECT	4472	5513	ND2	4536	OXPHOS Complex I
mt4820	ILLUMINA610	4472	5513	ND2	4536	OXPHOS Complex I
mt4824	ILLUMINA610	4472	5513	ND2	4536	OXPHOS Complex I
mt4883	ILLUMINA610	4472	5513	ND2	4536	OXPHOS Complex I
mt4917	DIRECT	4472	5513	ND2	4536	OXPHOS Complex I
mt4917	ILLUMINA610	4472	5513	ND2	4536	OXPHOS Complex I
mt4977	ILLUMINA610	4472	5513	ND2	4536	OXPHOS Complex I
mt5004	ILLUMINA610	4472	5513	ND2	4536	OXPHOS Complex I
mt5046	DIRECT	4472	5513	ND2	4536	OXPHOS Complex I
mt5046	ILLUMINA610	4472	5513	ND2	4536	OXPHOS Complex I
mt5147	DIRECT	4472	5513	ND2	4536	OXPHOS Complex I
mt5264	ILLUMINA610	4472	5513	ND2	4536	OXPHOS Complex I
mt5391	ILLUMINA610	4472	5513	ND2	4536	OXPHOS Complex I
mt5442	ILLUMINA610	4472	5513	ND2	4536	OXPHOS Complex I
mt5460	ILLUMINA610	4472	5513	ND2	4536	OXPHOS Complex I
mt5495	DIRECT	4472	5513	ND2	4536	OXPHOS Complex I
mt5495	ILLUMINA610	4472	5513	ND2	4536	OXPHOS Complex I
mt10238	DIRECT	10061	10406	ND3	4537	OXPHOS Complex I
mt10238	ILLUMINA610	10061	10406	ND3	4537	OXPHOS Complex I
mt10311	ILLUMINA610	10061	10406	ND3	4537	OXPHOS Complex I
mt10321	ILLUMINA610	10061	10406	ND3	4537	OXPHOS Complex I
mt10398	DIRECT	10061	10406	ND3	N/A	OXPHOS Complex I

Supplementary Table S2 (continued)

SNP	PLATFORM	START	END	GENE	ENTREZ	FUNCTION
mt10398	ILLUMINA610	10061	10406	ND3	N/A	OXPHOS Complex I
mt10463	ILLUMINA610	10407	10761	ND4L	4539	OXPHOS Complex I
mt10550	DIRECT	10407	10761	ND4L	4539	OXPHOS Complex I
mt10550	ILLUMINA610	10407	10761	ND4L	4539	OXPHOS Complex I
mt10586	ILLUMINA610	10407	10761	ND4L	4539	OXPHOS Complex I
mt10589	ILLUMINA610	10407	10761	ND4L	4539	OXPHOS Complex I
mt10688	ILLUMINA610	10407	10761	ND4L	4539	OXPHOS Complex I
mt10873	ILLUMINA610	10762	12139	ND4	4538	OXPHOS Complex I
mt10915	DIRECT	10762	12139	ND4	4538	OXPHOS Complex I
mt10915	ILLUMINA610	10762	12139	ND4	4538	OXPHOS Complex I
mt11251	DIRECT	10762	12139	ND4	4538	OXPHOS Complex I
mt11252	ILLUMINA610	10762	12139	ND4	4538	OXPHOS Complex I
mt11299	DIRECT	10762	12139	ND4	4538	OXPHOS Complex I
mt11377	DIRECT	10762	12139	ND4	4538	OXPHOS Complex I
mt11377	ILLUMINA610	10762	12139	ND4	4538	OXPHOS Complex I
mt11467	DIRECT	10762	12139	ND4	4538	OXPHOS Complex I
mt11467	ILLUMINA610	10762	12139	ND4	4538	OXPHOS Complex I
mt11485	DIRECT	10762	12139	ND4	4538	OXPHOS Complex I
mt11485	ILLUMINA610	10762	12139	ND4	4538	OXPHOS Complex I
mt11674	DIRECT	10762	12139	ND4	4538	OXPHOS Complex I
mt11719	DIRECT	10762	12139	ND4	4538	OXPHOS Complex I
mt11812	DIRECT	10762	12139	ND4	4538	OXPHOS Complex I
mt11900	ILLUMINA610	10762	12139	ND4	4538	OXPHOS Complex I
mt11914	DIRECT	10762	12139	ND4	4538	OXPHOS Complex I
mt11914	ILLUMINA610	10762	12139	ND4	4538	OXPHOS Complex I
mt11947	DIRECT	10762	12139	ND4	4538	OXPHOS Complex I
mt12007	DIRECT	10762	12139	ND4	4538	OXPHOS Complex I
mt12372	DIRECT	12339	14150	ND5	4540	OXPHOS Complex I
mt12372	ILLUMINA610	12339	14150	ND5	4540	OXPHOS Complex I

Supplementary Table S2 (continued)

SNP	PLATFORM	START	END	GENE	ENTREZ	FUNCTION
mt12414	DIRECT	12339	14150	ND5	4540	OXPHOS Complex I
mt12631	ILLUMINA610	12339	14150	ND5	4540	OXPHOS Complex I
mt12670	ILLUMINA610	12339	14150	ND5	4540	OXPHOS Complex I
mt12705	DIRECT	12339	14150	ND5	4540	OXPHOS Complex I
mt12705	ILLUMINA610	12339	14150	ND5	4540	OXPHOS Complex I
mt12851	ILLUMINA610	12339	14150	ND5	4540	OXPHOS Complex I
mt13020	DIRECT	12339	14150	ND5	4540	OXPHOS Complex I
mt13105	DIRECT	12339	14150	ND5	4540	OXPHOS Complex I
mt13105	ILLUMINA610	12339	14150	ND5	4540	OXPHOS Complex I
mt13263	ILLUMINA610	12339	14150	ND5	4540	OXPHOS Complex I
mt13368	DIRECT	12339	14150	ND5	4540	OXPHOS Complex I
mt13617	DIRECT	12339	14150	ND5	4540	OXPHOS Complex I
mt13650	ILLUMINA610	12339	14150	ND5	4540	OXPHOS Complex I
mt13708	DIRECT	12339	14150	ND5	4540	OXPHOS Complex I
mt13734	DIRECT	12339	14150	ND5	4540	OXPHOS Complex I
mt13780	DIRECT	12339	14150	ND5	4540	OXPHOS Complex I
mt13780	ILLUMINA610	12339	14150	ND5	4540	OXPHOS Complex I
mt13789	ILLUMINA610	12339	14150	ND5	4540	OXPHOS Complex I
mt13934	DIRECT	12339	14150	ND5	4540	OXPHOS Complex I
mt13965	DIRECT	12339	14150	ND5	4540	OXPHOS Complex I
mt13965	ILLUMINA610	12339	14150	ND5	4540	OXPHOS Complex I
mt13966	DIRECT	12339	14150	ND5	4540	OXPHOS Complex I
mt14167	DIRECT	14151	14675	ND6	4541	OXPHOS Complex I
mt14178	ILLUMINA610	14151	14675	ND6	4541	OXPHOS Complex I
mt14182	DIRECT	14151	14675	ND6	4541	OXPHOS Complex I
mt14233	DIRECT	14151	14675	ND6	4541	OXPHOS Complex I
mt14233	ILLUMINA610	14151	14675	ND6	4541	OXPHOS Complex I
mt14583	ILLUMINA610	14151	14675	ND6	4541	OXPHOS Complex I
mt14766	DIRECT	14749	15889	CYTB	4519	OXPHOS Complex III

Supplementary Table S2 (continued)

SNP	PLATFORM	START	END	GENE	ENTREZ	FUNCTION
mt14793	DIRECT	14749	15889	CYTB	4519	OXPPOS Complex III
mt14798	DIRECT	14749	15889	CYTB	4519	OXPPOS Complex III
mt14798	ILLUMINA610	14749	15889	CYTB	4519	OXPPOS Complex III
mt14905	DIRECT	14749	15889	CYTB	4519	OXPPOS Complex III
mt15043	DIRECT	14749	15889	CYTB	4519	OXPPOS Complex III
mt15043	ILLUMINA610	14749	15889	CYTB	4519	OXPPOS Complex III
mt15218	DIRECT	14749	15889	CYTB	4519	OXPPOS Complex III
mt15244	ILLUMINA610	14749	15889	CYTB	4519	OXPPOS Complex III
mt15257	DIRECT	14749	15889	CYTB	4519	OXPPOS Complex III
mt15257	ILLUMINA610	14749	15889	CYTB	4519	OXPPOS Complex III
mt15302	ILLUMINA610	14749	15889	CYTB	4519	OXPPOS Complex III
mt15452	DIRECT	14749	15889	CYTB	4519	OXPPOS Complex III
mt15535	ILLUMINA610	14749	15889	CYTB	4519	OXPPOS Complex III
mt15607	DIRECT	14749	15889	CYTB	4519	OXPPOS Complex III
mt15670	ILLUMINA610	14749	15889	CYTB	4519	OXPPOS Complex III
mt15758	DIRECT	14749	15889	CYTB	4519	OXPPOS Complex III
mt15758	ILLUMINA610	14749	15889	CYTB	4519	OXPPOS Complex III
mt15784	ILLUMINA610	14749	15889	CYTB	4519	OXPPOS Complex III
mt15833	DIRECT	14749	15889	CYTB	4519	OXPPOS Complex III
mt15833	ILLUMINA610	14749	15889	CYTB	4519	OXPPOS Complex III
mt5951	ILLUMINA610	5906	7447	COX1	4512	OXPPOS Complex IV
mt6027	ILLUMINA610	5906	7447	COX1	4512	OXPPOS Complex IV
mt6046	ILLUMINA610	5906	7447	COX1	4512	OXPPOS Complex IV
mt6153	ILLUMINA610	5906	7447	COX1	4512	OXPPOS Complex IV
mt6221	DIRECT	5906	7447	COX1	4512	OXPPOS Complex IV
mt6221	ILLUMINA610	5906	7447	COX1	4512	OXPPOS Complex IV
mt6260	ILLUMINA610	5906	7447	COX1	4512	OXPPOS Complex IV
mt6681	ILLUMINA610	5906	7447	COX1	4512	OXPPOS Complex IV
mt6735	ILLUMINA610	5906	7447	COX1	4512	OXPPOS Complex IV
mt6753	ILLUMINA610	5906	7447	COX1	4512	OXPPOS Complex IV
mt6776	DIRECT	5906	7447	COX1	4512	OXPPOS Complex IV
mt6776	ILLUMINA610	5906	7447	COX1	4512	OXPPOS Complex IV

Supplementary Table S2 (continued)

SNP	PLATFORM	START	END	GENE	ENTREZ	FUNCTION
mt7028	DIRECT	5906	7447	COX1	4512	OXPHOS Complex IV
mt7055	ILLUMINA610	5906	7447	COX1	4512	OXPHOS Complex IV
mt7175	ILLUMINA610	5906	7447	COX1	4512	OXPHOS Complex IV
mt7274	ILLUMINA610	5906	7447	COX1	4512	OXPHOS Complex IV
mt7768	DIRECT	7588	8271	COX2	4513	OXPHOS Complex IV
mt7769	ILLUMINA610	7588	8271	COX2	4513	OXPHOS Complex IV
mt8251	DIRECT	7588	8271	COX2	4513	OXPHOS Complex IV
mt8269	ILLUMINA610	7588	8271	COX2	4513	OXPHOS Complex IV
mt9378	ILLUMINA610	9210	9992	COX3	4514	OXPHOS Complex IV
mt9477	DIRECT	9210	9992	COX3	4514	OXPHOS Complex IV
mt9540	ILLUMINA610	9210	9992	COX3	4514	OXPHOS Complex IV
mt9667	DIRECT	9210	9992	COX3	4514	OXPHOS Complex IV
mt9667	ILLUMINA610	9210	9992	COX3	4514	OXPHOS Complex IV
mt9698	DIRECT	9210	9992	COX3	4514	OXPHOS Complex IV
mt9698	ILLUMINA610	9210	9992	COX3	4514	OXPHOS Complex IV
mt9716	DIRECT	9210	9992	COX3	4514	OXPHOS Complex IV
mt9716	ILLUMINA610	9210	9992	COX3	4514	OXPHOS Complex IV
mt9899	DIRECT	9210	9992	COX3	4514	OXPHOS Complex IV
mt9899	ILLUMINA610	9210	9992	COX3	4514	OXPHOS Complex IV
mt9950	ILLUMINA610	9210	9992	COX3	4514	OXPHOS Complex IV
mt8617	ILLUMINA610	8529	9209	ATP6	4508	OXPHOS Complex V
mt8655	ILLUMINA610	8529	9209	ATP6	4508	OXPHOS Complex V
mt8697	DIRECT	8529	9209	ATP6	4508	OXPHOS Complex V
mt8869	ILLUMINA610	8529	9209	ATP6	4508	OXPHOS Complex V
mt8994	DIRECT	8529	9209	ATP6	4508	OXPHOS Complex V
mt9055	DIRECT	8529	9209	ATP6	4508	OXPHOS Complex V
mt9072	ILLUMINA610	8529	9209	ATP6	4508	OXPHOS Complex V
mt9094	ILLUMINA610	8529	9209	ATP6	4508	OXPHOS Complex V
mt9123	DIRECT	8529	9209	ATP6	4508	OXPHOS Complex V

Supplementary Table S2 (continued)

SNP	PLATFORM	START	END	GENE	ENTREZ	FUNCTION
mt16130	ILLUMINA610	15996	16571	Noncoding	N/A	Unknown
mt16145	ILLUMINA610	15996	16571	Noncoding	N/A	Unknown
mt16146	ILLUMINA610	15996	16571	Noncoding	N/A	Unknown
mt16149	ILLUMINA610	15996	16571	Noncoding	N/A	Unknown
mt16163	ILLUMINA610	15996	16571	Noncoding	N/A	Unknown
mt16164	ILLUMINA610	15996	16571	Noncoding	N/A	Unknown
mt16184	ILLUMINA610	15996	16571	Noncoding	N/A	Unknown
mt16189	DIRECT	15996	16571	Noncoding	N/A	Unknown
mt16272	ILLUMINA610	15996	16571	Noncoding	N/A	Unknown
mt16329	ILLUMINA610	15996	16571	Noncoding	N/A	Unknown
mt16392	ILLUMINA610	15996	16571	Noncoding	N/A	Unknown
mt16393	ILLUMINA610	15996	16571	Noncoding	N/A	Unknown

Platform data extracted for Illumina 610 microarray. Directly genotyped SNPs according to previously published protocols reported as DIRECT. ENTREZ = Entrez Gene ID, OXHOS = oxidative phosphorylation, SNP = single nucleotide polymorphism



Supplementary Table S3. Beta associations for risk of all-cause ischemic stroke in the MGH/MIGen discovery cohort for genotyped autosomal and mitochondrial variants

<b>SNP</b>	<b>MITO_or_AUTO</b>	<b>MT_POS</b>	<b>ALLELE_CODED</b>	<b>BETA_WEIGHT</b>
mt217	MITO	217	T	-0.0011
mt228	MITO	228	A	0.00511
mt247	MITO	247	A	-0.0073
mt295	MITO	295	T	0.00543
mt458	MITO	458	T	-0.0002
mt464	MITO	464	T	0.0067
mt479	MITO	479	T	0.0067
mt491	MITO	491	T	-0.0086
mt750	MITO	750	A	0.10165
mt827	MITO	827	A	0.00657
mt1048	MITO	1048	T	0.0019
mt1189	MITO	1189	T	-0.0395
mt1438	MITO	1438	A	0.00035
mt1719	MITO	1719	A	-0.1366
mt1736	MITO	1736	A	-0.0052
mt2160	MITO	2160	T	0.00513
mt2485	MITO	2485	T	-0.0037
mt2706	MITO	2706	A	0.24998
mt2789	MITO	2789	T	0.0046
mt2885	MITO	2885	T	-0.0073
mt3010	MITO	3010	A	-0.034
mt3197	MITO	3197	T	0.02078
mt3348	MITO	3348	A	0.00465
mt3394	MITO	3394	T	0.17563
mt3480	MITO	3480	A	-0.2115
mt3594	MITO	3594	T	0.00896
mt3666	MITO	3666	A	-0.0069
mt3721	MITO	3721	A	0.00467
mt3915	MITO	3915	A	-0.0776
mt3918	MITO	3918	A	-0.0046
mt3971	MITO	3971	T	-0.0051
mt3993	MITO	3993	T	-0.0024
mt4025	MITO	4025	A	0.0055
mt4336	MITO	4336	C	-0.0068
mt4769	MITO	4769	A	-0.0112

SNP	MITO_or_AUTO	MT_POS	ALLELE_CODED	BETA_WEIGHT
mt4820	MITO	4820	A	0.00039
mt4824	MITO	4824	A	0.00154
mt4883	MITO	4883	T	-0.0116
mt4917	MITO	4917	G	0.02664
mt4977	MITO	4977	T	0.00405
mt5004	MITO	5004	T	-0.0021
mt5046	MITO	5046	G	-0.0309
mt5264	MITO	5264	T	-0.0018
mt5391	MITO	5391	A	0.00528
mt5442	MITO	5442	T	-0.0036
mt5460	MITO	5460	A	0.0012
mt5495	MITO	5495	C	-0.0185
mt5773	MITO	5773	A	-0.0056
mt5951	MITO	5951	A	-0.0007
mt6027	MITO	6027	A	-0.007
mt6046	MITO	6046	T	0.00414
mt6153	MITO	6153	T	-0.0012
mt6221	MITO	6221	C	-0.2054
mt6260	MITO	6260	A	-0.0101
mt6681	MITO	6681	T	-0.0014
mt6735	MITO	6735	A	-0.0112
mt6753	MITO	6753	A	-0.0016
mt6776	MITO	6776	C	0.07232
mt7055	MITO	7055	A	0.00829
mt7175	MITO	7175	T	0.00284
mt7274	MITO	7274	T	-0.0016
mt7769	MITO	7769	A	0.00943
mt8269	MITO	8269	A	-0.0011
mt8278	MITO	8278	T	0.00635
mt8617	MITO	8617	T	-0.0051
mt8655	MITO	8655	T	-0.004
mt8869	MITO	8869	A	0.00664
mt9072	MITO	9072	A	-0.0037
mt9094	MITO	9094	A	-0.0148
mt9378	MITO	9378	A	-0.0048
mt9540	MITO	9540	T	-0.0047
mt9667	MITO	9667	G	0.09349
mt9698	MITO	9698	C	-0.2115

SNP	MITO_or_AUTO	MT_POS	ALLELE_CODED	BETA_WEIGHT
mt9716	MITO	9716	C	-0.1099
mt9899	MITO	9899	C	0.08158
mt9950	MITO	9950	T	-0.0037
mt10034	MITO	10034	T	0.00995
mt10045	MITO	10045	A	-0.0025
mt10238	MITO	10238	T	0.00299
mt10311	MITO	10311	A	-0.0006
mt10321	MITO	10321	T	-0.0048
mt10398	MITO	10398	G	0.1319
mt10463	MITO	10463	T	-0.0008
mt10550	MITO	10550	G	-0.2115
mt10586	MITO	10586	A	-0.003
mt10589	MITO	10589	A	0.00127
mt10688	MITO	10688	A	-6.6291
mt10873	MITO	10873	T	0.00253
mt10915	MITO	10915	C	0.30968
mt11252	MITO	11252	A	0.00304
mt11377	MITO	11377	A	-0.026
mt11467	MITO	11467	A	-0.014
mt11485	MITO	11485	C	-0.0497
mt11900	MITO	11900	T	0.00032
mt11914	MITO	11914	A	-0.0821
mt12309	MITO	12309	A	0.00386
mt12372	MITO	12372	A	-0.0475
mt12631	MITO	12631	A	-0.0015
mt12670	MITO	12670	T	0.00952
mt12705	MITO	12705	T	-0.1504
mt12851	MITO	12851	A	0.01453
mt13105	MITO	13105	G	-0.1351
mt13263	MITO	13263	A	0.00629
mt13650	MITO	13650	T	0.00732
mt13780	MITO	13780	A	0.06765
mt13789	MITO	13789	T	-0.0027
mt13965	MITO	13965	C	-0.0577
mt14178	MITO	14178	T	0.09352
mt14233	MITO	14233	G	-0.1961
mt14583	MITO	14583	A	-0.0984
mt14798	MITO	14798	C	-0.0263

SNP	MITO_or_AUTO	MT_POS	ALLELE_CODED	BETA_WEIGHT
mt15043	MITO	15043	A	-0.0061
mt15244	MITO	15244	A	-0.0001
mt15257	MITO	15257	A	0.10345
mt15302	MITO	15302	A	0.00898
mt15535	MITO	15535	T	0.00493
mt15670	MITO	15670	T	0.00779
mt15758	MITO	15758	G	-0.0216
mt15784	MITO	15784	T	-0.0012
mt15833	MITO	15833	T	0.03343
mt15904	MITO	15904	C	-0.1536
mt15924	MITO	15924	A	-0.0135
mt15928	MITO	15928	A	0.02664
mt15931	MITO	15931	A	-0.0027
mt16130	MITO	16130	A	-0.0103
mt16145	MITO	16145	T	0.01576
mt16146	MITO	16146	A	-0.0086
mt16149	MITO	16149	T	-0.0043
mt16163	MITO	16163	A	0.00161
mt16164	MITO	16164	A	0.00475
mt16184	MITO	16184	A	-0.0045
mt16272	MITO	16272	T	0.00398
mt16329	MITO	16329	T	-0.0001
mt16392	MITO	16392	A	0.0021
mt16393	MITO	16393	A	0.00354
rs6693480	AUTO	n/a	A	0.0422
rs12085482	AUTO	n/a	G	-0.3057
rs1883911	AUTO	n/a	T	-0.3799
rs6681946	AUTO	n/a	G	0.0104
rs2454160	AUTO	n/a	A	0.0069
rs2454161	AUTO	n/a	T	0.0080
rs2454162	AUTO	n/a	T	0.0080
rs2454163	AUTO	n/a	T	0.0104
rs2454165	AUTO	n/a	C	-0.0245
rs2454170	AUTO	n/a	T	0.0080
rs2501810	AUTO	n/a	T	-0.0343
rs2935931	AUTO	n/a	T	-0.2035
rs3003452	AUTO	n/a	C	-0.2035
rs2977265	AUTO	n/a	A	-0.1987

SNP	MITO_or_AUTO	MT_POS	ALLELE_CODED	BETA_WEIGHT
rs3003456	AUTO	n/a	A	-0.2035
rs16826012	AUTO	n/a	C	0.0653
rs4660208	AUTO	n/a	G	0.0696
rs2246160	AUTO	n/a	A	0.3271
rs7542296	AUTO	n/a	C	-0.0056
rs12138736	AUTO	n/a	C	-0.0111
rs3737741	AUTO	n/a	C	-0.0106
rs11588450	AUTO	n/a	C	-0.0144
rs2476163	AUTO	n/a	G	0.0167
rs2486166	AUTO	n/a	T	-0.0154
rs2211012	AUTO	n/a	T	0.1202
rs4233505	AUTO	n/a	G	-0.2281
rs17665274	AUTO	n/a	C	-0.2452
rs692801	AUTO	n/a	G	0.1339
rs2746444	AUTO	n/a	C	-0.4632
rs571020	AUTO	n/a	G	0.1216
rs11576942	AUTO	n/a	T	-0.0125
rs10776734	AUTO	n/a	T	0.3069
rs2067552	AUTO	n/a	T	0.5490
rs9943162	AUTO	n/a	G	0.0975
rs10799885	AUTO	n/a	C	0.1234
rs6681091	AUTO	n/a	G	0.1315
rs2343491	AUTO	n/a	C	-0.0106
rs6659661	AUTO	n/a	G	-0.0159
rs12091621	AUTO	n/a	G	0.0694
rs4512621	AUTO	n/a	C	0.3862
rs2661275	AUTO	n/a	T	-0.0961
rs2661274	AUTO	n/a	C	-0.0841
rs951437	AUTO	n/a	T	-0.0175
rs951438	AUTO	n/a	T	-0.0175
rs2842028	AUTO	n/a	A	0.0421
rs12043369	AUTO	n/a	A	0.1044
rs2661315	AUTO	n/a	T	0.0274
rs11578512	AUTO	n/a	A	-0.2537
rs11578513	AUTO	n/a	A	-0.2537
rs2841957	AUTO	n/a	T	-0.0592
rs16849162	AUTO	n/a	C	0.8848
rs2661314	AUTO	n/a	C	0.0488

SNP	MITO_or_AUTO	MT_POS	ALLELE_CODED	BETA_WEIGHT
rs2063142	AUTO	n/a	G	-0.0598
rs2841958	AUTO	n/a	A	0.0379
rs2661303	AUTO	n/a	T	0.0297
rs7606070	AUTO	n/a	C	0.0829
rs17493655	AUTO	n/a	A	0.0811
rs1879954	AUTO	n/a	C	0.0713
rs16863205	AUTO	n/a	A	0.0736
rs2437904	AUTO	n/a	T	0.4808
rs2037528	AUTO	n/a	C	0.0736
rs11681616	AUTO	n/a	G	-0.1373
rs11898629	AUTO	n/a	T	-0.1112
rs1448905	AUTO	n/a	C	0.0833
rs1947200	AUTO	n/a	T	0.0119
rs755024	AUTO	n/a	C	-0.1667
rs2279687	AUTO	n/a	C	0.0681
rs7595693	AUTO	n/a	T	0.0590
rs12695010	AUTO	n/a	A	-0.1191
rs1565986	AUTO	n/a	T	0.0689
rs1009283	AUTO	n/a	T	0.0599
rs10191103	AUTO	n/a	C	0.4593
rs12105315	AUTO	n/a	C	0.4998
rs6742692	AUTO	n/a	T	0.5192
rs1603326	AUTO	n/a	A	-0.0891
rs1845775	AUTO	n/a	C	0.4998
rs1495921	AUTO	n/a	A	-0.0934
rs10170009	AUTO	n/a	T	-0.0891
rs11685173	AUTO	n/a	C	-0.1351
rs7589895	AUTO	n/a	A	-0.1415
rs7608911	AUTO	n/a	C	-0.1427
rs7592893	AUTO	n/a	A	-0.1390
rs4417745	AUTO	n/a	G	0.0953
rs7608790	AUTO	n/a	G	-0.1493
rs7597153	AUTO	n/a	A	-0.1427
rs13034435	AUTO	n/a	T	0.0098
rs6739663	AUTO	n/a	A	0.1076
rs4854077	AUTO	n/a	A	0.1392
rs12623425	AUTO	n/a	T	0.0196
rs4854076	AUTO	n/a	G	0.0926

SNP	MITO_or_AUTO	MT_POS	ALLELE_CODED	BETA_WEIGHT
rs1106154	AUTO	n/a	A	-0.0323
rs12695014	AUTO	n/a	A	0.0763
rs952753	AUTO	n/a	A	0.1466
rs4854033	AUTO	n/a	T	0.0871
rs7607116	AUTO	n/a	G	0.1029
rs7573172	AUTO	n/a	T	0.0741
rs10933588	AUTO	n/a	C	0.0144
rs11685834	AUTO	n/a	C	-0.0252
rs6746446	AUTO	n/a	G	0.0119
rs6437322	AUTO	n/a	A	0.0667
rs7565424	AUTO	n/a	A	0.0254
rs11688673	AUTO	n/a	T	-0.0252
rs7420288	AUTO	n/a	G	0.0574
rs2352821	AUTO	n/a	T	0.0269
rs7602820	AUTO	n/a	A	-0.0134
rs12997738	AUTO	n/a	G	-0.0141
rs2352838	AUTO	n/a	T	-0.2687
rs7579238	AUTO	n/a	A	-0.2965
rs11677104	AUTO	n/a	T	-0.3021
rs12996674	AUTO	n/a	G	0.3446
rs10174868	AUTO	n/a	T	-0.2687
rs6437325	AUTO	n/a	A	-0.2394
rs10178014	AUTO	n/a	G	-0.1454
rs10933595	AUTO	n/a	G	-0.2432
rs1320123	AUTO	n/a	G	-0.1743
rs4676439	AUTO	n/a	T	-0.2894
rs4571052	AUTO	n/a	G	-0.3029
rs11885409	AUTO	n/a	T	-0.2777
rs10165842	AUTO	n/a	A	-0.2777
rs13063312	AUTO	n/a	A	-0.2128
rs7631574	AUTO	n/a	T	-0.2477
rs2276852	AUTO	n/a	G	-0.2477
rs3821876	AUTO	n/a	T	-0.2128
rs13324142	AUTO	n/a	T	-0.2243
rs2276850	AUTO	n/a	A	-0.2243
rs740787	AUTO	n/a	G	-0.2477
rs2310996	AUTO	n/a	C	-0.2477
rs6438441	AUTO	n/a	A	-0.1902

SNP	MITO_or_AUTO	MT_POS	ALLELE_CODED	BETA_WEIGHT
rs1486336	AUTO	n/a	T	0.0130
rs6779584	AUTO	n/a	G	-0.0838
rs6767666	AUTO	n/a	T	-0.0373
rs1032292	AUTO	n/a	C	-0.3730
rs1032291	AUTO	n/a	T	-0.3573
rs9828139	AUTO	n/a	C	-0.3611
rs9823302	AUTO	n/a	A	-0.3611
rs1489626	AUTO	n/a	G	-0.3297
rs28648408	AUTO	n/a	C	-0.0326
rs6840253	AUTO	n/a	G	0.2908
rs315312	AUTO	n/a	T	-0.0749
rs221592	AUTO	n/a	G	-0.0809
rs4398492	AUTO	n/a	C	-0.0749
rs11728884	AUTO	n/a	C	0.0460
rs2126207	AUTO	n/a	C	0.0327
rs17882175	AUTO	n/a	A	-0.0456
rs6841713	AUTO	n/a	A	-0.3278
rs12503968	AUTO	n/a	G	0.1034
rs6535865	AUTO	n/a	G	-0.3278
rs17050688	AUTO	n/a	C	0.0146
rs1108867	AUTO	n/a	T	-0.2184
rs6889904	AUTO	n/a	C	-0.1142
rs2059861	AUTO	n/a	T	-0.2567
rs7700533	AUTO	n/a	T	-0.1142
rs7717734	AUTO	n/a	T	-0.1915
rs7717970	AUTO	n/a	T	-0.2318
rs11133847	AUTO	n/a	A	-0.2318
rs4956990	AUTO	n/a	A	-0.1894
rs13176160	AUTO	n/a	A	-0.2318
rs4956991	AUTO	n/a	A	-0.1918
rs1053477	AUTO	n/a	C	-0.2318
rs4956993	AUTO	n/a	A	-0.1963
rs1053478	AUTO	n/a	A	-0.2318
rs1053479	AUTO	n/a	A	-0.2318
rs7727015	AUTO	n/a	C	-0.1723
rs6861289	AUTO	n/a	T	-0.2318
rs4956994	AUTO	n/a	G	-0.2700
rs10040260	AUTO	n/a	C	0.0335



SNP	MITO_or_AUTO	MT_POS	ALLELE_CODED	BETA_WEIGHT
rs13174204	AUTO	n/a	C	0.0592
rs16884543	AUTO	n/a	G	-0.0102
rs10512651	AUTO	n/a	G	-0.1151
rs12516704	AUTO	n/a	C	-0.0020
rs10065003	AUTO	n/a	C	0.3619
rs6872379	AUTO	n/a	G	0.0783
rs9790964	AUTO	n/a	A	0.3617
rs16881474	AUTO	n/a	A	0.3538
rs1991002	AUTO	n/a	G	0.0728
rs1532163	AUTO	n/a	A	-0.0437
rs1532162	AUTO	n/a	T	0.0114
rs923610	AUTO	n/a	G	0.0114
rs7728496	AUTO	n/a	T	-0.0532
rs7717681	AUTO	n/a	C	0.0114
rs256107	AUTO	n/a	G	-0.0398
rs10036010	AUTO	n/a	G	0.1067
rs1994648	AUTO	n/a	G	-0.0095
rs2637002	AUTO	n/a	A	0.0096
rs403207	AUTO	n/a	G	-0.0509
rs424955	AUTO	n/a	A	-0.0520
rs423872	AUTO	n/a	C	0.0197
rs365578	AUTO	n/a	T	0.0614
rs31304	AUTO	n/a	A	-0.0544
rs31303	AUTO	n/a	A	-0.0382
rs31302	AUTO	n/a	C	0.0197
rs976630	AUTO	n/a	C	-0.0089
rs4647078	AUTO	n/a	A	0.0884
rs976080	AUTO	n/a	A	0.1463
rs158570	AUTO	n/a	C	0.0035
rs158928	AUTO	n/a	G	0.1147
rs158935	AUTO	n/a	C	0.0035
rs158572	AUTO	n/a	G	0.0063
rs4647028	AUTO	n/a	T	-0.0930
rs158919	AUTO	n/a	T	0.0035
rs158916	AUTO	n/a	G	0.1064
rs158914	AUTO	n/a	G	-0.0633
rs158926	AUTO	n/a	T	0.0977
rs158923	AUTO	n/a	C	0.0003

SNP	MITO_or_AUTO	MT_POS	ALLELE_CODED	BETA_WEIGHT
rs158563	AUTO	n/a	C	0.0938
rs1609041	AUTO	n/a	T	0.0977
rs1382914	AUTO	n/a	G	0.0035
rs3101879	AUTO	n/a	G	-0.0633
rs2650517	AUTO	n/a	G	0.0035
rs7723901	AUTO	n/a	T	-0.0495
rs167912	AUTO	n/a	A	0.0868
rs290505	AUTO	n/a	T	0.1166
rs290506	AUTO	n/a	A	0.0003
rs162242	AUTO	n/a	G	-0.0096
rs162240	AUTO	n/a	A	0.0640
rs329614	AUTO	n/a	G	0.0978
rs12655209	AUTO	n/a	C	-0.0495
rs17419290	AUTO	n/a	G	-0.0089
rs162231	AUTO	n/a	G	0.0938
rs162235	AUTO	n/a	C	0.0978
rs248688	AUTO	n/a	T	-0.0660
rs34592	AUTO	n/a	C	-0.0492
rs726824	AUTO	n/a	G	-0.0376
rs34638	AUTO	n/a	G	-0.0492
rs248685	AUTO	n/a	G	-0.0032
rs248682	AUTO	n/a	C	-0.0022
rs16878547	AUTO	n/a	C	0.1054
rs10471502	AUTO	n/a	A	-0.0592
rs295533	AUTO	n/a	A	-0.0022
rs295531	AUTO	n/a	G	-0.0592
rs295561	AUTO	n/a	T	-0.0488
rs295559	AUTO	n/a	A	-0.0592
rs1460961	AUTO	n/a	G	-0.0178
rs4308511	AUTO	n/a	T	1.2350
rs13177204	AUTO	n/a	G	0.0499
rs803217	AUTO	n/a	G	0.0331
rs778597	AUTO	n/a	A	-0.1116
rs2563335	AUTO	n/a	A	-0.0836
rs240414	AUTO	n/a	G	-0.1434
rs743004	AUTO	n/a	C	-0.1952
rs3777510	AUTO	n/a	T	-0.2047
rs240433	AUTO	n/a	A	-0.1910

SNP	MITO_or_AUTO	MT_POS	ALLELE_CODED	BETA_WEIGHT
rs997875	AUTO	n/a	T	-0.1821
rs213858	AUTO	n/a	C	-0.1000
rs9372215	AUTO	n/a	C	-0.2107
rs9487145	AUTO	n/a	C	0.0223
rs10484996	AUTO	n/a	T	-0.0562
rs399454	AUTO	n/a	G	0.2582
rs1640705	AUTO	n/a	A	0.0068
rs218983	AUTO	n/a	G	0.0035
rs6956814	AUTO	n/a	C	0.1067
rs10263162	AUTO	n/a	C	0.0829
rs2523075	AUTO	n/a	A	0.1016
rs2717900	AUTO	n/a	A	0.1174
rs12538022	AUTO	n/a	T	0.1847
rs2523073	AUTO	n/a	G	0.1058
rs12535348	AUTO	n/a	C	0.1847
rs10256921	AUTO	n/a	C	0.0854
rs7792939	AUTO	n/a	C	0.0280
rs3735453	AUTO	n/a	C	0.1584
rs1506642	AUTO	n/a	G	-0.1683
rs17146312	AUTO	n/a	G	0.1092
rs608447	AUTO	n/a	A	-0.1683
rs600774	AUTO	n/a	A	0.0826
rs627689	AUTO	n/a	A	-0.1789
rs659416	AUTO	n/a	A	0.0808
rs9886090	AUTO	n/a	A	0.1423
rs2079978	AUTO	n/a	T	-0.2593
rs801122	AUTO	n/a	A	-0.1772
rs488795	AUTO	n/a	T	-0.0786
rs512509	AUTO	n/a	T	-0.0753
rs4726225	AUTO	n/a	A	-0.1661
rs471817	AUTO	n/a	A	-0.0753
rs528957	AUTO	n/a	T	-0.0753
rs498933	AUTO	n/a	A	-0.1451
rs7005317	AUTO	n/a	T	-0.2165
rs7834966	AUTO	n/a	G	0.0980
rs11784299	AUTO	n/a	C	0.0980
rs10956927	AUTO	n/a	A	0.0980
rs11996455	AUTO	n/a	A	-0.0718

SNP	MITO_or_AUTO	MT_POS	ALLELE_CODED	BETA_WEIGHT
rs13271375	AUTO	n/a	G	-0.0718
rs13271644	AUTO	n/a	A	0.0100
rs16917079	AUTO	n/a	G	0.0980
rs6986418	AUTO	n/a	G	0.2377
rs7009086	AUTO	n/a	A	0.7056
rs10441538	AUTO	n/a	G	0.0099
rs6471499	AUTO	n/a	A	-0.2185
rs6989591	AUTO	n/a	C	0.0980
rs11782617	AUTO	n/a	T	0.0980
rs6991067	AUTO	n/a	G	-0.0755
rs7004862	AUTO	n/a	G	-0.0718
rs713113	AUTO	n/a	T	-0.0043
rs6471500	AUTO	n/a	G	-0.2185
rs16917102	AUTO	n/a	T	0.2377
rs7844932	AUTO	n/a	G	0.2312
rs10956929	AUTO	n/a	C	-0.2209
rs7009940	AUTO	n/a	G	0.2312
rs2278891	AUTO	n/a	G	-0.2214
rs16893774	AUTO	n/a	C	-0.0001
rs28399553	AUTO	n/a	G	-0.0001
rs16917117	AUTO	n/a	C	-0.0001
rs550564	AUTO	n/a	A	-0.1942
rs2956216	AUTO	n/a	T	-0.2327
rs7015841	AUTO	n/a	A	-0.0297
rs7017487	AUTO	n/a	C	-0.0136
rs683832	AUTO	n/a	T	-0.2078
rs551270	AUTO	n/a	T	-0.2385
rs13264488	AUTO	n/a	T	0.0465
rs10956931	AUTO	n/a	T	-0.1128
rs2123647	AUTO	n/a	G	-0.0005
rs12548874	AUTO	n/a	A	-0.0383
rs2945554	AUTO	n/a	C	-0.0118
rs10956932	AUTO	n/a	A	-0.0118
rs1011796	AUTO	n/a	C	-0.0369
rs11784717	AUTO	n/a	T	-0.1325
rs9643353	AUTO	n/a	C	-0.0401
rs524678	AUTO	n/a	T	-0.1658
rs493506	AUTO	n/a	G	-0.1623

SNP	MITO_or_AUTO	MT_POS	ALLELE_CODED	BETA_WEIGHT
rs1453377	AUTO	n/a	C	-0.1278
rs1453379	AUTO	n/a	T	-0.1996
rs4735336	AUTO	n/a	G	-0.0588
rs16893776	AUTO	n/a	C	-0.1266
rs4735339	AUTO	n/a	C	-0.1263
rs11782818	AUTO	n/a	C	0.0684
rs11778553	AUTO	n/a	T	0.0684
rs11783878	AUTO	n/a	C	0.0661
rs12549003	AUTO	n/a	A	-0.2032
rs7827478	AUTO	n/a	T	-0.2079
rs10086284	AUTO	n/a	A	-0.1893
rs3802193	AUTO	n/a	T	-0.2071
rs3802191	AUTO	n/a	G	0.0661
rs10098778	AUTO	n/a	C	-0.0673
rs2514530	AUTO	n/a	T	-0.0454
rs2514531	AUTO	n/a	C	-0.0461
rs1788150	AUTO	n/a	T	0.0873
rs16897728	AUTO	n/a	A	0.0826
rs921313	AUTO	n/a	A	0.1190
rs2442756	AUTO	n/a	C	0.0734
rs10956185	AUTO	n/a	G	0.0231
rs3812472	AUTO	n/a	G	0.0619
rs4330675	AUTO	n/a	T	-0.3933
rs9100	AUTO	n/a	T	0.1895
rs6558292	AUTO	n/a	A	0.4419
rs673710	AUTO	n/a	G	-0.0593
rs10971028	AUTO	n/a	C	0.2214
rs629566	AUTO	n/a	C	-0.0414
rs653790	AUTO	n/a	T	-0.0399
rs700083	AUTO	n/a	T	0.1272
rs700084	AUTO	n/a	A	0.6396
rs700085	AUTO	n/a	T	0.0416
rs700086	AUTO	n/a	T	0.1166
rs700088	AUTO	n/a	T	0.1216
rs3824534	AUTO	n/a	A	0.6396
rs4292757	AUTO	n/a	A	0.0181
rs7023064	AUTO	n/a	A	0.0714
rs11255332	AUTO	n/a	C	0.0520

SNP	MITO_or_AUTO	MT_POS	ALLELE_CODED	BETA_WEIGHT
rs11255333	AUTO	n/a	A	-0.1117
rs7342066	AUTO	n/a	A	0.1028
rs11255338	AUTO	n/a	G	0.1037
rs1555961	AUTO	n/a	G	0.1123
rs2026612	AUTO	n/a	T	0.1286
rs11596873	AUTO	n/a	A	0.1330
rs2269195	AUTO	n/a	T	-0.0731
rs2269196	AUTO	n/a	C	0.0082
rs10786568	AUTO	n/a	T	0.1893
rs6584321	AUTO	n/a	C	0.1684
rs1998289	AUTO	n/a	C	0.1598
rs1998290	AUTO	n/a	G	0.1709
rs767844	AUTO	n/a	G	-0.2565
rs2295779	AUTO	n/a	G	-0.0806
rs10883509	AUTO	n/a	T	-0.0806
rs4919471	AUTO	n/a	G	-0.0937
rs10883511	AUTO	n/a	G	-0.0806
rs4752856	AUTO	n/a	A	0.2210
rs11231726	AUTO	n/a	T	0.0660
rs4930224	AUTO	n/a	T	-0.1038
rs308314	AUTO	n/a	T	-0.0412
rs1979579	AUTO	n/a	C	0.1727
rs634918	AUTO	n/a	G	0.1958
rs7112234	AUTO	n/a	A	-0.4036
rs7939646	AUTO	n/a	C	-0.4040
rs4529911	AUTO	n/a	C	0.0425
rs11214256	AUTO	n/a	T	0.1117
rs7119817	AUTO	n/a	C	-0.1700
rs7105881	AUTO	n/a	T	-0.1725
rs7108821	AUTO	n/a	A	-0.1725
rs10891394	AUTO	n/a	T	0.1324
rs12287565	AUTO	n/a	C	0.2507
rs9788072	AUTO	n/a	G	-0.2104
rs9788097	AUTO	n/a	G	-0.2316
rs1860345	AUTO	n/a	C	0.0877
rs4765787	AUTO	n/a	T	-0.0136
rs12821926	AUTO	n/a	T	-0.0850
rs2239503	AUTO	n/a	C	0.1643

SNP	MITO_or_AUTO	MT_POS	ALLELE_CODED	BETA_WEIGHT
rs2239504	AUTO	n/a	C	0.1660
rs2239505	AUTO	n/a	T	-0.0427
rs965186	AUTO	n/a	G	0.2589
rs12582005	AUTO	n/a	A	-0.2562
rs10747750	AUTO	n/a	C	-0.0502
rs931552	AUTO	n/a	A	0.0386
rs1881655	AUTO	n/a	C	0.0235
rs1729798	AUTO	n/a	C	0.0236
rs11172551	AUTO	n/a	G	0.1199
rs1795708	AUTO	n/a	C	-0.1747
rs1729790	AUTO	n/a	C	0.1735
rs11172556	AUTO	n/a	C	0.1199
rs7974886	AUTO	n/a	G	-0.0393
rs10877107	AUTO	n/a	A	0.1199
rs12424252	AUTO	n/a	G	0.1199
rs4337085	AUTO	n/a	G	0.1119
rs11108526	AUTO	n/a	T	-0.4996
rs10777797	AUTO	n/a	T	-0.4510
rs12426901	AUTO	n/a	A	-0.2077
rs935031	AUTO	n/a	A	-0.4707
rs11108532	AUTO	n/a	C	0.1139
rs7953936	AUTO	n/a	T	0.0906
rs7967631	AUTO	n/a	T	-0.0519
rs7954377	AUTO	n/a	C	-0.0227
rs10860041	AUTO	n/a	G	-0.0237
rs10860042	AUTO	n/a	C	-0.0228
rs12582303	AUTO	n/a	C	-0.0242
rs7132929	AUTO	n/a	T	-0.4940
rs7139277	AUTO	n/a	G	0.2561
rs6571530	AUTO	n/a	T	0.0632
rs17412060	AUTO	n/a	A	0.0273
rs17412116	AUTO	n/a	A	0.0273
rs2224429	AUTO	n/a	G	0.0765
rs10147478	AUTO	n/a	A	-0.1509
rs1956993	AUTO	n/a	G	0.1630
rs17099187	AUTO	n/a	C	-0.1588
rs8006810	AUTO	n/a	C	-0.0539
rs6571531	AUTO	n/a	T	-0.0539

SNP	MITO_or_AUTO	MT_POS	ALLELE_CODED	BETA_WEIGHT
rs3742925	AUTO	n/a	G	-0.0319
rs1998242	AUTO	n/a	A	-0.0003
rs2224266	AUTO	n/a	A	-0.0002
rs17099235	AUTO	n/a	C	0.1556
rs3742926	AUTO	n/a	T	0.1556
rs17099240	AUTO	n/a	G	0.1556
rs2383340	AUTO	n/a	A	0.1556
rs9635189	AUTO	n/a	G	0.1421
rs17099246	AUTO	n/a	C	0.1385
rs1956204	AUTO	n/a	T	0.0345
rs6571535	AUTO	n/a	A	0.0340
rs2891205	AUTO	n/a	A	0.0595
rs17099276	AUTO	n/a	T	0.4384
rs8012268	AUTO	n/a	T	0.0595
rs11846766	AUTO	n/a	G	0.4384
rs17099285	AUTO	n/a	G	0.4384
rs17414154	AUTO	n/a	A	-0.1033
rs1950702	AUTO	n/a	A	0.1113
rs11626762	AUTO	n/a	G	-0.0588
rs12435734	AUTO	n/a	A	0.0199
rs1956210	AUTO	n/a	T	0.0033
rs8016916	AUTO	n/a	A	-0.1543
rs8017249	AUTO	n/a	T	0.0091
rs1950703	AUTO	n/a	A	-0.1292
rs768787	AUTO	n/a	T	-0.0807
rs17099322	AUTO	n/a	C	-0.0657
rs1956212	AUTO	n/a	A	0.0158
rs1956214	AUTO	n/a	C	0.0005
rs733978	AUTO	n/a	T	-0.0131
rs4981990	AUTO	n/a	A	0.0493
rs4981991	AUTO	n/a	G	0.0685
rs12887176	AUTO	n/a	T	0.0685
rs10483416	AUTO	n/a	G	-0.0611
rs1956221	AUTO	n/a	A	-0.0176
rs1956223	AUTO	n/a	T	-0.0611
rs4981992	AUTO	n/a	A	0.0095
rs927062	AUTO	n/a	G	-0.0568
rs11627900	AUTO	n/a	G	-0.0792



SNP	MITO_or_AUTO	MT_POS	ALLELE_CODED	BETA_WEIGHT
rs17515243	AUTO	n/a	C	-0.0209
rs6571547	AUTO	n/a	T	-0.0038
rs10141122	AUTO	n/a	C	-0.0178
rs12437429	AUTO	n/a	A	-0.0332
rs11627566	AUTO	n/a	C	0.0081
rs10135053	AUTO	n/a	A	0.0040
rs10135562	AUTO	n/a	T	-0.0286
rs6571548	AUTO	n/a	C	0.0548
rs1884621	AUTO	n/a	T	-0.1547
rs10139964	AUTO	n/a	T	-0.0820
rs4981997	AUTO	n/a	C	0.0401
rs17099434	AUTO	n/a	C	-0.0189
rs1884622	AUTO	n/a	T	0.0009
rs1028537	AUTO	n/a	G	0.0020
rs1950698	AUTO	n/a	T	0.0737
rs10134827	AUTO	n/a	A	0.0272
rs1956208	AUTO	n/a	C	0.0737
rs12892900	AUTO	n/a	T	0.0737
rs7156205	AUTO	n/a	G	0.0020
rs3742929	AUTO	n/a	C	0.0020
rs8013508	AUTO	n/a	A	0.0737
rs970662	AUTO	n/a	A	-0.0701
rs12431588	AUTO	n/a	T	0.0737
rs1955512	AUTO	n/a	G	0.1344
rs1295912	AUTO	n/a	C	-0.1667
rs981524	AUTO	n/a	C	-0.1554
rs1955491	AUTO	n/a	C	0.1817
rs4981999	AUTO	n/a	T	-0.1658
rs1950221	AUTO	n/a	C	0.1124
rs10149509	AUTO	n/a	C	-0.1276
rs3784209	AUTO	n/a	A	0.1400
rs2300830	AUTO	n/a	C	0.1400
rs2239646	AUTO	n/a	G	0.0107
rs2300831	AUTO	n/a	G	-0.1276
rs4982002	AUTO	n/a	T	-0.1803
rs2300832	AUTO	n/a	A	-0.1803
rs2300833	AUTO	n/a	A	-0.1803
rs17440692	AUTO	n/a	C	-0.1216

SNP	MITO_or_AUTO	MT_POS	ALLELE_CODED	BETA_WEIGHT
rs2300837	AUTO	n/a	G	-0.1803
rs12890485	AUTO	n/a	G	-0.0337
rs7159774	AUTO	n/a	C	0.2855
rs17091663	AUTO	n/a	A	-0.0348
rs1955507	AUTO	n/a	A	-0.0835
rs9788573	AUTO	n/a	A	-0.0017
rs7141509	AUTO	n/a	G	0.2849
rs4982005	AUTO	n/a	G	-0.0470
rs8012632	AUTO	n/a	T	-0.0366
rs17519834	AUTO	n/a	A	-0.2534
rs2273163	AUTO	n/a	T	-0.0032
rs11845042	AUTO	n/a	A	0.2690
rs17441370	AUTO	n/a	T	-0.1686
rs10144064	AUTO	n/a	T	0.2777
rs926771	AUTO	n/a	T	0.2402
rs10131032	AUTO	n/a	A	0.2402
rs7146681	AUTO	n/a	G	-0.0460
rs17099538	AUTO	n/a	C	0.2303
rs2383377	AUTO	n/a	A	0.0838
rs6572739	AUTO	n/a	C	0.0330
rs7161242	AUTO	n/a	T	-0.0481
rs4271523	AUTO	n/a	C	0.2031
rs9672038	AUTO	n/a	C	-0.1217
rs4901097	AUTO	n/a	G	-0.0454
rs4264315	AUTO	n/a	A	-0.1287
rs8006468	AUTO	n/a	A	0.0416
rs4901098	AUTO	n/a	A	0.0801
rs2447196	AUTO	n/a	A	0.0833
rs28495368	AUTO	n/a	A	0.1203
rs2260160	AUTO	n/a	T	0.0149
rs16968681	AUTO	n/a	C	-0.1720
rs11637488	AUTO	n/a	C	-0.0406
rs17653749	AUTO	n/a	A	0.1694
rs3211995	AUTO	n/a	A	-0.0733
rs1017228	AUTO	n/a	C	-0.0083
rs4783438	AUTO	n/a	T	-0.0263
rs9921702	AUTO	n/a	A	-0.0263
rs11649675	AUTO	n/a	G	0.0039

SNP	MITO_or_AUTO	MT_POS	ALLELE_CODED	BETA_WEIGHT
rs1862648	AUTO	n/a	C	0.0004
rs9788908	AUTO	n/a	A	-0.0083
rs7190264	AUTO	n/a	T	-0.2089
rs35635	AUTO	n/a	G	0.0595
rs4384614	AUTO	n/a	A	0.1060
rs13332445	AUTO	n/a	A	-0.0964
rs8079640	AUTO	n/a	A	-0.0875
rs12943936	AUTO	n/a	A	-0.0569
rs16949067	AUTO	n/a	G	0.1989
rs17616525	AUTO	n/a	A	0.0709
rs9891372	AUTO	n/a	C	-0.0815
rs17616591	AUTO	n/a	G	-0.0387
rs11652402	AUTO	n/a	A	0.0709
rs8073382	AUTO	n/a	A	-0.0206
rs3785680	AUTO	n/a	A	0.0478
rs2323093	AUTO	n/a	C	-0.0407
rs12449610	AUTO	n/a	C	-0.0206
rs2323095	AUTO	n/a	G	-0.0206
rs2323097	AUTO	n/a	G	-0.0206
rs8070339	AUTO	n/a	G	-0.0206
rs2530377	AUTO	n/a	A	-0.0206
rs2530376	AUTO	n/a	G	-0.0206
rs12453877	AUTO	n/a	G	0.0344
rs2529626	AUTO	n/a	A	-0.0620
rs917309	AUTO	n/a	T	-0.0620
rs3826366	AUTO	n/a	C	0.0515
rs9901549	AUTO	n/a	C	0.0515
rs11078233	AUTO	n/a	C	-0.0465
rs11078234	AUTO	n/a	G	-0.0620
rs7214082	AUTO	n/a	A	-0.0620
rs1802618	AUTO	n/a	C	-0.0611
rs1050216	AUTO	n/a	C	-0.0611
rs9907078	AUTO	n/a	G	-0.1174
rs8077212	AUTO	n/a	C	0.1996
rs988489	AUTO	n/a	T	0.1959
rs2874992	AUTO	n/a	C	0.1996
rs7207687	AUTO	n/a	C	0.1959
rs11654370	AUTO	n/a	A	0.1960

SNP	MITO_or_AUTO	MT_POS	ALLELE_CODED	BETA_WEIGHT
rs9895549	AUTO	n/a	G	0.2027
rs9897617	AUTO	n/a	C	0.2052
rs9903896	AUTO	n/a	G	-0.1683
rs1859904	AUTO	n/a	T	-0.1233
rs17680043	AUTO	n/a	A	-0.1086
rs7503943	AUTO	n/a	A	0.2060
rs11078237	AUTO	n/a	G	0.0009
rs16949314	AUTO	n/a	A	-0.0852
rs11868525	AUTO	n/a	T	-0.0661
rs16949319	AUTO	n/a	G	0.0841
rs960296	AUTO	n/a	G	-0.2036
rs7217154	AUTO	n/a	T	-0.1574
rs4426402	AUTO	n/a	C	-0.2283
rs12943914	AUTO	n/a	G	-0.2239
rs10445283	AUTO	n/a	G	-0.1888
rs4794258	AUTO	n/a	T	0.0727
rs7226040	AUTO	n/a	G	-0.1609
rs2970020	AUTO	n/a	C	-0.2317
rs16950939	AUTO	n/a	G	0.0008
rs11867634	AUTO	n/a	A	-0.0556
rs7217314	AUTO	n/a	C	-0.1065
rs11658103	AUTO	n/a	T	-0.0841
rs12601604	AUTO	n/a	C	-0.0459
rs12600934	AUTO	n/a	C	0.3914
rs1785560	AUTO	n/a	C	-0.0515
rs874250	AUTO	n/a	T	-0.0449
rs12966444	AUTO	n/a	A	0.1607
rs11660603	AUTO	n/a	G	-0.0449
rs4798772	AUTO	n/a	G	0.0021
rs1792670	AUTO	n/a	C	-0.0645
rs1792668	AUTO	n/a	G	-0.0872
rs729112	AUTO	n/a	A	-0.0715
rs2012555	AUTO	n/a	T	-0.1006
rs11082638	AUTO	n/a	T	-0.0663
rs1539872	AUTO	n/a	C	-0.0832
rs12488	AUTO	n/a	T	0.2031
rs10423270	AUTO	n/a	G	-0.1796
rs7251937	AUTO	n/a	C	-0.0628

SNP	MITO_or_AUTO	MT_POS	ALLELE_CODED	BETA_WEIGHT
rs4807125	AUTO	n/a	T	-0.2868
rs2967605	AUTO	n/a	T	-0.0419
rs17160489	AUTO	n/a	G	0.0129
rs12983092	AUTO	n/a	T	0.0620
rs6511744	AUTO	n/a	G	-0.1179
rs4804628	AUTO	n/a	G	-0.1085
rs4804629	AUTO	n/a	C	-0.1179
rs4804631	AUTO	n/a	C	-0.1085
rs7252405	AUTO	n/a	G	-0.1085
rs7258257	AUTO	n/a	A	-0.1085
rs8101160	AUTO	n/a	C	-0.1036
rs4808319	AUTO	n/a	G	-0.0614
rs4809215	AUTO	n/a	G	-0.0352
rs11667828	AUTO	n/a	G	0.1640
rs919778	AUTO	n/a	A	0.1775
rs1609034	AUTO	n/a	G	0.1727
rs2198978	AUTO	n/a	T	0.2263
rs10500244	AUTO	n/a	T	0.0428
rs2052572	AUTO	n/a	A	0.0456
rs10425998	AUTO	n/a	T	0.0467
rs11671438	AUTO	n/a	T	0.0448
rs34486765	AUTO	n/a	A	0.0801
rs9676602	AUTO	n/a	G	-0.0082
rs6121376	AUTO	n/a	A	0.0410
rs2830535	AUTO	n/a	C	0.2477
rs455633	AUTO	n/a	C	-0.0867
rs464273	AUTO	n/a	T	-0.0835
rs457752	AUTO	n/a	T	0.2385
rs7278046	AUTO	n/a	T	0.1853
rs457864	AUTO	n/a	A	-0.0284
rs2830538	AUTO	n/a	C	0.2276
rs461307	AUTO	n/a	A	-0.0941
rs458546	AUTO	n/a	C	-0.0941
rs463433	AUTO	n/a	A	0.2601
rs465401	AUTO	n/a	A	0.2050
rs460420	AUTO	n/a	T	0.2168
rs12483589	AUTO	n/a	A	0.1746
rs2830544	AUTO	n/a	T	0.1792

SNP	MITO_or_AUTO	MT_POS	ALLELE_CODED	BETA_WEIGHT
rs2834714	AUTO	n/a	C	-0.1019
rs990115	AUTO	n/a	T	-0.1048
rs1008882	AUTO	n/a	G	-0.0804
rs2834716	AUTO	n/a	A	-0.1565
rs2834719	AUTO	n/a	T	-0.0305
rs8129743	AUTO	n/a	T	-0.0305
rs2242880	AUTO	n/a	T	-0.0305
rs737234	AUTO	n/a	T	-0.0305
rs9977678	AUTO	n/a	A	-0.0305
rs9306172	AUTO	n/a	C	-0.0042
rs2838475	AUTO	n/a	T	0.1528
rs2299817	AUTO	n/a	T	-0.1281
rs2255828	AUTO	n/a	T	0.0286
rs2245462	AUTO	n/a	C	0.0037
rs915877	AUTO	n/a	G	0.1982
rs2071152	AUTO	n/a	A	0.0037
rs2838486	AUTO	n/a	G	0.0270
rs1131999	AUTO	n/a	C	0.0538
rs17004630	AUTO	n/a	A	-0.0419
rs2277806	AUTO	n/a	C	0.0156
rs7277269	AUTO	n/a	C	-0.0071
rs2020945	AUTO	n/a	G	-0.0050
rs2243999	AUTO	n/a	C	0.0156
rs756554	AUTO	n/a	C	0.0156
rs2071142	AUTO	n/a	G	0.0156
rs2071143	AUTO	n/a	A	0.0156
rs2187313	AUTO	n/a	T	0.0136
rs2838490	AUTO	n/a	C	0.0156
rs2251267	AUTO	n/a	T	0.0151
rs968714	AUTO	n/a	T	0.0156
rs2838491	AUTO	n/a	G	0.0156
rs4819376	AUTO	n/a	C	0.0156
rs4819382	AUTO	n/a	T	0.0554
rs7283041	AUTO	n/a	A	0.0544
rs2838503	AUTO	n/a	G	0.0186
rs2838506	AUTO	n/a	A	0.1260
rs2838508	AUTO	n/a	G	0.0945
rs2838512	AUTO	n/a	C	-0.0491

<b>SNP</b>	<b>MITO_or_AUTO</b>	<b>MT_POS</b>	<b>ALLELE_CODED</b>	<b>BETA_WEIGHT</b>
rs12628465	AUTO	n/a	G	0.0282
rs4823094	AUTO	n/a	A	-0.0779
rs1894629	AUTO	n/a	T	-0.0779
rs17327536	AUTO	n/a	C	0.0593
rs5953019	AUTO	n/a	T	0.0279
rs2227291	AUTO	n/a	C	0.1688
rs17139617	AUTO	n/a	A	0.1848
rs7063278	AUTO	n/a	T	-0.0023
rs1468422	AUTO	n/a	C	0.4859

Supplementary Table S4. Statistical power to discover association between individual OXPPOS genetic variants and ischemic stroke, based on available sample size and odds ratios conferring increased ischemic stroke risk, assuming an additive model

Phenotype	MAF	OR		
		1.10	1.20	1.40
All Ischemic Stroke	0.10	0.001	0.013	0.25
	0.20	0.003	0.046	0.59
	0.30	0.004	0.079	0.73
Small Vessel	0.10	< 0.001	0.002	0.03
	0.20	< 0.001	0.005	0.08
	0.30	< 0.001	0.007	0.11

Alpha =  $6 \times 10^{-5}$  (842 independent tests). MAF = minor allele frequency, OR = odds ratio, OXPPOS = oxidative phosphorylation



Supplementary Table S5. Statistical power to discover association between OXPPOS genetic risk score and ischemic stroke and intracerebral hemorrhage, based on available sample size and % of variance explained

Phenotype	% Variance Explained		
	0.5%	1%	5%
All Ischemic Stroke	0.21	0.57	0.99
- Cardioembolic	0.04	0.48	0.80
- Large Artery	0.03	0.43	0.78
- Small Vessel	0.03	0.41	0.77
All ICH	0.16	0.54	0.88
- Lobar ICH	0.08	0.50	0.84
- Deep ICH	0.08	0.50	0.85

Alpha = 0.0125 (4 independent tests) for ischemic stroke. Alpha = 0.0166 (3 independent tests) for ICH. ICH = Intracerebral Hemorrhage, OXPPOS = oxidative phosphorylation

Supplementary Table S6. Change in odds ratio point estimates and p-values from Table 3 with omission of mitochondrial variants from the genetic score

	All OXPHOS		Complex I		Complex IV	
	OR	p	OR	p	OR	p
All ischemic stroke	1.17 (- 13%)	0.008 <b>(0.006)</b>	1.06 (-20%)	0.050 <b>(0.062)</b>	1.05 (- 11%)	0.075 <b>(0.11)</b>
SV	1.16 (- 18%)	0.007 <b>(0.01)</b>	1.13 (- 12%)	0.027 <b>(0.033)</b>	1.14 (- 9%)	0.018 <b>(0.018)</b>
All ICH	---	---	---	---	1.08 (-10%)	0.039 <b>(0.043)</b>
Deep ICH	---	---	---	---	1.14 (-7%)	0.008 <b>(0.008)</b>

Re-presentation of Table 3 in the original manuscript, with percent change in odds ratio and new p-values for each test with the omission of mitochondrial variants from the genetic score in bold. ICH = intracerebral hemorrhage, OR = odds ratio, SV = small vessel stroke.